Development of Simulation-Based Method for Benefit Estimation of Automatic Emergency Braking and Lane Departure Warning in Traffic Collisions

Mitsuaki Goto
Nana Takeuchi
Takao Matsuda
Yuichi Kitagawa
Toyota Motor Corporation
Japan

Paper Number 23-0039

ABSTRACT

In this study, a simulation-based method was developed for benefit estimation of Automatic Emergency Braking (AEB) and Lane Departure Warning (LDW). The collision avoidance effect and the injury mitigation effect of AEB and LDW were probabilistically estimated through large-scale simulations of near-miss scenarios leading to traffic collisions. The top nine near-miss scenarios were selected from the fatal collision data in Japan. The simulation parameters such as vehicle speed and its position in the lane were varied based on the statistical data to realistically simulate various situations in the field. A total of 17,000 simulations were conducted for each with or without AEB or LDW in order to calculate the reduction of collisions cases. For the collision cases, crash simulations were conducted using a virtual human body model "THUMS" to predict the fatality risk. In this study, the head injury value, HIC_{15}, was used to determine whether the injury level was fatal. The benefit of AEB/LDW was estimated by multiplying their effect for each collision scenario by the percentage of the scenarios in the total number of fatal collisions in Japan. When neither AEB nor LDW were activated, collisions occurred in 117,031 out of 153,000 cases. When AEB or LDW was activated, collisions occurred in 48,030 cases. The collision avoidance effect by AEB or LDW was estimated to be 59.0 %. In the collision cases, there were 415 fatal cases where AEB was not activated while in 76 cases with AEB was activated. Based on the results, the injury mitigation effect was estimated to be 81.5 %. The simulation results for the top nine scenarios indicated 29.9 % for the benefit in collision avoidance and 52.4 % for the benefit in injury mitigation.

INTRODUCTION

Advanced driver-assistance systems (ADAS) are becoming widespread in many countries. The system alerts the driver when it detects a risk of collision. AEB activates the brakes when the driver does not apply the brakes despite the presence of a collision risk. The system tries to avoid the collision and mitigate the damage by lowering the vehicle speed. LDW alerts the driver when the vehicle is about to depart from the lane for some reason such as distraction. It tries to avoid the collisions with an oncoming vehicle or obstacles such as guard rails. The performance of ADAS functions is evaluated in vehicle tests under prescribed conditions assuming common collision scenarios [1-3]. The performance tests of AEB in Euro NCAP are conducted on the target assuming near-miss situations with pedestrians, bicycles, and vehicles ahead. The AEB rating for pedestrians assumes that pedestrians are crossing. The test scores are calculated from the result of 110 test cases with different vehicle speed, direction of pedestrian, presence of blind spots, and day/night conditions. However, there could be many types of actual collision scenarios. This makes it difficult to quantitatively estimate the effectiveness of ADAS in the field. Previous study reported the performance of ADAS in actual traffic conditions based on the past accident database [4]. It takes several years to accumulate the necessary number of accident data for such a study. It is difficult to predict the effectiveness of new safety features under development. Few studies have quantitatively investigated the effectiveness of ADAS on human injury mitigation. The objective of this study is to develop a simulation-based method to estimate the effectiveness of AEB and LDW in terms of collision avoidance and injury mitigation, considering the variation traffic collisions. The benefit of AEB and LDW in fatal collisions is also estimated at the national level using this method.

METHOD

The effectiveness of AEB and LDW was estimated by combining two simulations: vehicle dynamics simulation and crash simulation. The purpose of vehicle dynamics simulation was to estimate the reduction in the number of collision cases by activating AEB. The purpose of crash simulation was to estimate the reduction in the number of fatalities (Figure 1) in collision cases. For AEB, the effectiveness in both collision avoidance and injury mitigation was estimated. For LDW, the collision avoidance effect was estimated. Note that LDW works to prevent lane departure.

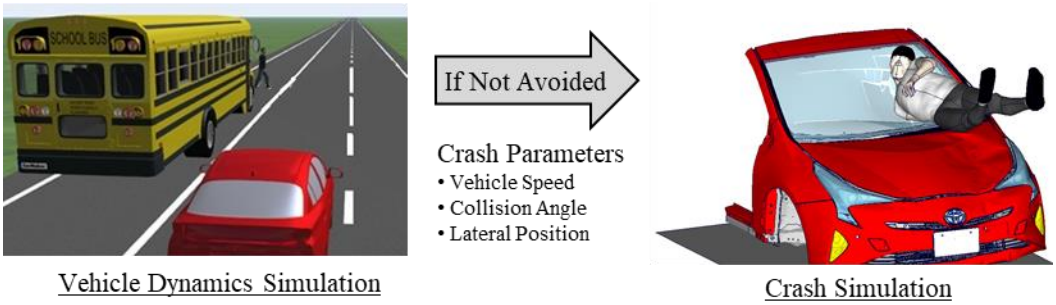

Figure 1. Simulations for estimating effectiveness of AEB and LDW.

Vehicle Dynamics Simulation

The vehicle dynamics simulations assumed various near-miss scenarios that could lead to collisions. The simulations were conducted assuming top nine fatal collision scenarios in the traffic collision database in Japan (Table 1). The top nine scenarios are pedestrian crossing, collision with a bicycle or a motorcycle at an intersection, collision when the vehicle was turning right or left, single-vehicle collision, and head-on collision. It accounted for approximately 80% of fatal traffic collisions reported in Japan [5]. The pedestrian crossing assumed the scenario (i) where a pedestrian appeared from the blind spot of a parked vehicle. Intersection scenarios assumed situations where bicycle (scenario (ii)) or motorcycle (scenario (iii)) entered the intersection from the crossing road. The right/left turn scenarios assumed the situations where the turning vehicle came close to a pedestrian (scenario (iv), (vi)) or a bicycle (scenario (v), (vii)) moving in the same direction or the opposite direction. The single-vehicle collision assumed the scenarios where the vehicle departed from the lane and came close to obstacles such as guard rails and a pole. The other case assumed a head-on collision with an oncoming vehicle. In each scenario, parameters such as vehicle speed/position, pedestrian walking speed/direction, those of bicycle/motorcycle, other road environment features were stochastically varied based on actual statistical data [6-11] and human behavioral characteristics to represent the variety in actual traffic collisions. A total of 17,000 simulation cases were generated for each scenario (Figure 2, Table 2). A pair of the simulation sets were performed with and without AEB/LDW. A total of 153,000 (17,000 cases for each of the nine scenarios) simulations were conducted in this study. The reduction of collision cases by AEB/LDW was calculated for each scenario. The benefit of AEB/LDW was estimated by multiplying the effectiveness of AEB/LDW in each scenario by the percentage of the scenario in the total number of fatal collisions in Japan. The effectiveness of AEB was estimated for the scenarios of pedestrian crossing and right/left turning at intersections. The effectiveness of LDW was estimated for the scenarios of single vehicle collision and head-on collision. The simulation model assumed a medium-sized sedan as the subject vehicle. The vehicle model replicated a real vehicle with a sensor and brake performance. The AEB model was added to the vehicle model to activate the brakes when the time to collision (TTC) with an object fell below a threshold value. The field of view was set to the range where the view angle of the millimeter wave radar and the monocular camera overlapped (46deg). The driving environment was assumed to be daytime on a sunny day. It was assumed that the object was detected as soon as it entered the field of view. There was no additional time (latency) between the detection and the initiation of braking. Assuming the dry condition for the road surface, a constant braking deceleration was defined for AEB model with the maximum jerk of 16.7 m/s^3 and the maximum deceleration of 9.8 m/s^2 as shown in Figure 3(a). A human driver model was used for the cases where AEB was not activated. The braking operation was simulated considering individual differences (Figure 3(b)). Based on the volunteer test data [12], the variation in idle time (0.2 ~ 5.1s), jerk (0.5~16.7m/s^3) and maximum deceleration (0.5~9.8m/s^2) were reproduced in the human driver model. The field of view was assumed to be 100 degrees. The driver detected the object as soon as it entered the field of view. In the right/left turning scenarios without AEB, it was assumed that the driver missed detecting the obstacle despite it entered in the field of view. As for LDW, the system alerted the driver when the vehicle deviated from the center of the lane and approached an obstacle. The driver model

was designed to return to the center of the lane after hearing the alert. Based on the volunteer test data [13], the variations in reaction time (0.3~2.1s), steering angular velocity (0~320deg/s) and maximum steering angle (0~160deg) were reproduced (Figure 4) in the driver model. In the cases without LDW, the vehicle continued the motion without appropriate steering operation to stay in the lane. CarMaker of IPG Automotive was used for vehicle driving simulation. The simulation models of AEB, LDW, and the human driver were developed in MATLAB/Simulink from MathWorks and incorporated into CarMaker's vehicle model.

Table 1.
Simulation scenarios.

No.	Collision Scenario	Description	ADAS	Number of Simulations
(i)	Pedestrian Crossing	Crossing - Pedestrian from left/right side	AEB	17,000
			-	17,000
(ii)	Bicyclist Crossing	Crossing - Bicyclist from oncoming bicycle lane left/right and straight	AEB	17,000
			-	17,000
(iii)	Motorcyclist Crossing	Crossing - Motorcyclist from left/right and driving straight	AEB	17,000
			-	17,000
(iv)	Pedestrian in right-turn	Right turning vehicle and pedestrian in same/opposite direction	AEB	17,000
			-	17,000
(v)	Bicyclist in right-turn	Right turning vehicle and bicyclist from bicycle lane in same/opposite direction	AEB	17,000
			-	17,000
(vi)	Pedestrian in left-turn	Left turning vehicle and pedestrian in same/opposite direction	AEB	17,000
			-	17,000
(vii)	Bicyclist in left-turn	Left turning vehicle and bicyclist from bicycle lane in same/opposite direction	AEB	17,000
			-	17,000
(viii)	Single-Vehicle Collision	Other accident - Fix obstacle	LDW	17,000
			-	17,000
(ix)	Head-on Collision with Vehicle	Head on - Encountering vehicles in curve	LDW	17,000
			-	17,000
Total				153,000 × 2

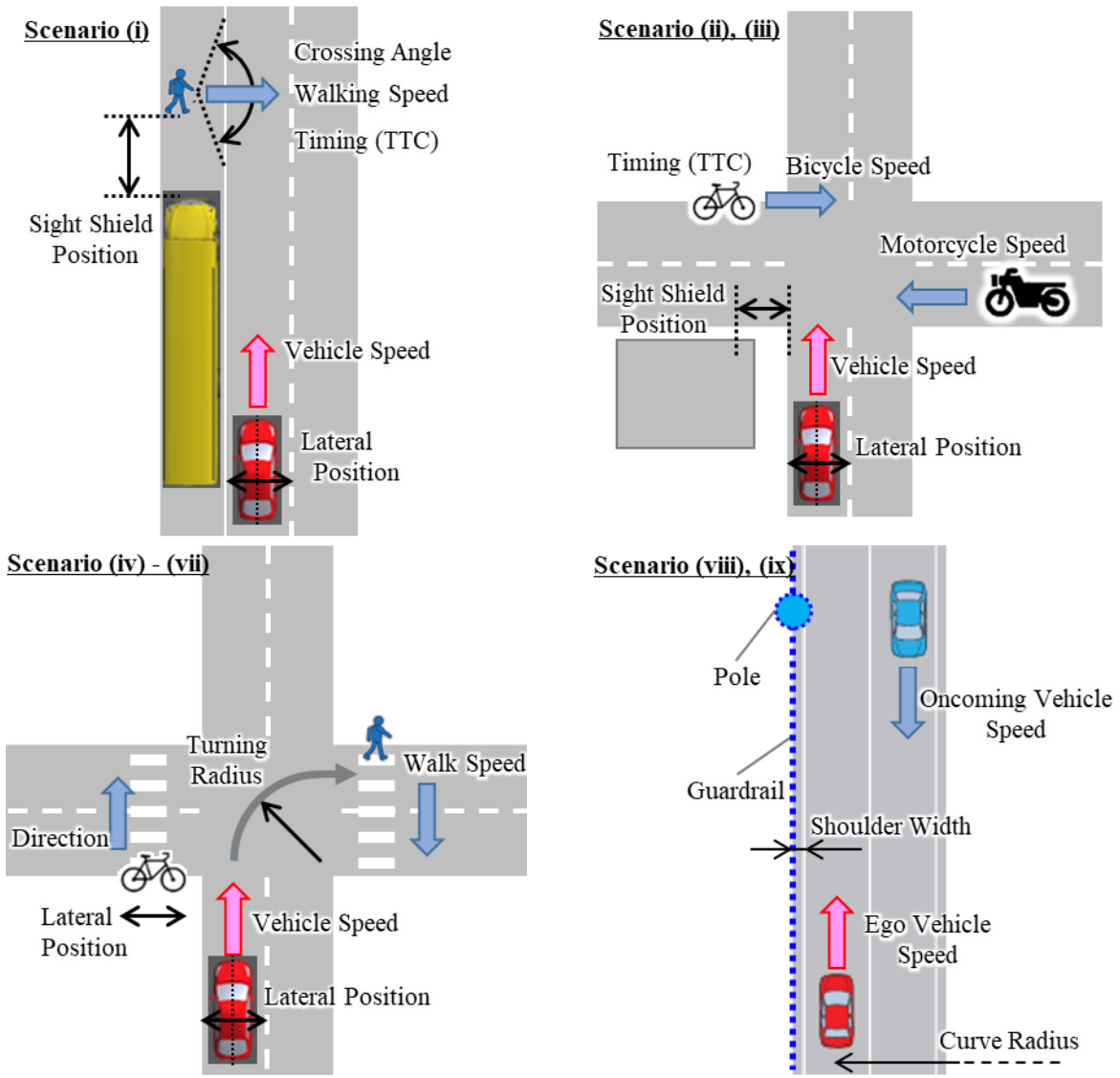

Figure 2. Simulation scenarios.

Table 2.
Simulation parameters and ranges.

No.	Collision Scenario	Parameter		Unit	Range	Distribution
(i)	Pedestrian Crossing	Pedestrian	Speed	m/s	0.8 - 2.0	Gaussian
			Crossing Angle	deg.	-70 - +70	Gaussian
			Timing	s	0.7 - 10	Log-normal
		Vehicle	Speed	km/h	10 - 60	Gaussian
			Lateral Position	m	-0.8 - +0.8	Gaussian
		Others	Sight Shield Position	m	4 - 24	Logarithmic
(ii)	Bicyclist Crossing	Bicyclist	Speed	km/h	3 - 21	Uniform
			Lateral Position	-	Sidewalk/Bicycle Lane	Uniform
			Direction	-	Left/Right	Uniform
			Timing	s	-0.2 - +0.2	Uniform
		Vehicle	Speed	km/h	10 - 60	Uniform
			Lateral Position	m	-0.8 - +0.8	Uniform
		Others	Sight Shield Position	m	0 - 35	Uniform
(iii)	Motorcyclist Crossing	Motorcyclist	Speed	km/h	10 - 60	Uniform
			Lateral Position	-	Roadway	Uniform
			Direction	-	Left/Right	Uniform
			Timing	s	-0.2 - +0.2	Uniform
		Vehicle	same as (ii)			
		Others	same as (ii)			
(iv)	Pedestrian in Right-Turn	Pedestrian	Speed	km/h	3 - 8	Gaussian
			Lateral Position	m	-0.5 - +0.5	Uniform
			Direction	-	Same/Opposite	Uniform
		Vehicle	Speed	km/h	12 - 36	Gaussian
			Turning Radius	m	5 - 10/5 - 16	Gaussian
			Lateral Position	m	-0.8 - +0.8	Uniform
(v)	Bicyclist in Right-Turn	Bicyclist				
			Lateral Position	m	-0.5 - +0.5	Uniform
			Direction	deg	Same/Opposite	Uniform
		Vehicle	Speed	km/h	12 - 36	Gaussian
			Turning Radius	m	5 - 10/5 - 16	Gaussian
			Lateral Position	m	-0.8 - +0.8	Uniform
(vi)	Pedestrian in Left-Turn	Pedestrian	same as (iv)			
		Vehicle	same as (iv)			
(vii)	Bicyclist in Left-Turn	Bicyclist	same as (v)			
		Vehicle	same as (v)			
(viii)	Single-Vehicle Collision	Vehicle	Speed	km/h	50 - 80	Gaussian
			Departure Angle	deg	0 - 25/0 - 30	Gaussian
		Road	Curve Radius	m	150 - 1050/Straight	Log-normal
			Shoulder Width	m	0.5/0.75	-
		Other	Fix Obstacle	-	Pole/Guardrail	Uniform
(ix)	Head-on Collision with Vehicle	Ego Vehicle	Speed	km/h	50 - 80	Gaussian
			Departure Angle	deg	0 - 25/0 - 30	Gaussian
		Oncoming Vehicle	Speed	km/h	0 - 80	Gaussian
		Road	Curve Radius	m	150 - 1050/Straight	Log-normal

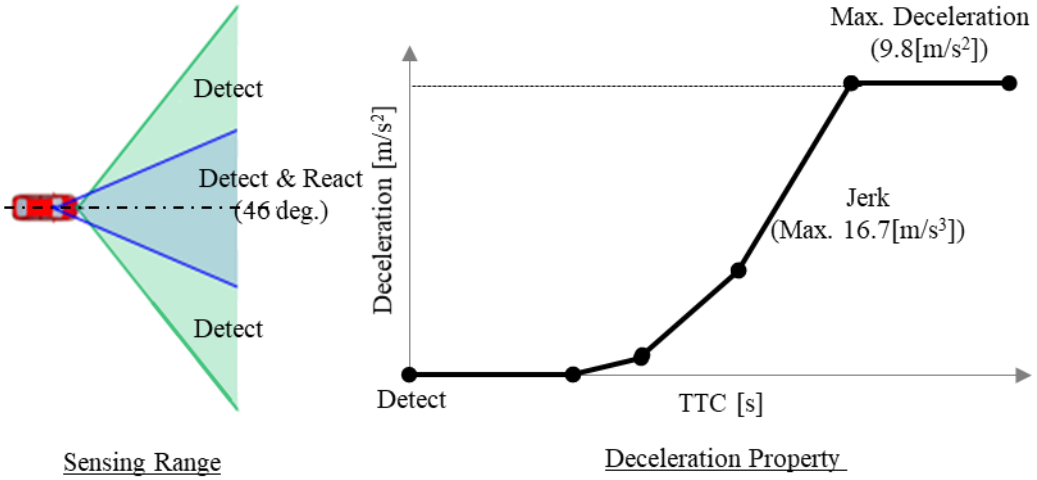

(a) AEB model

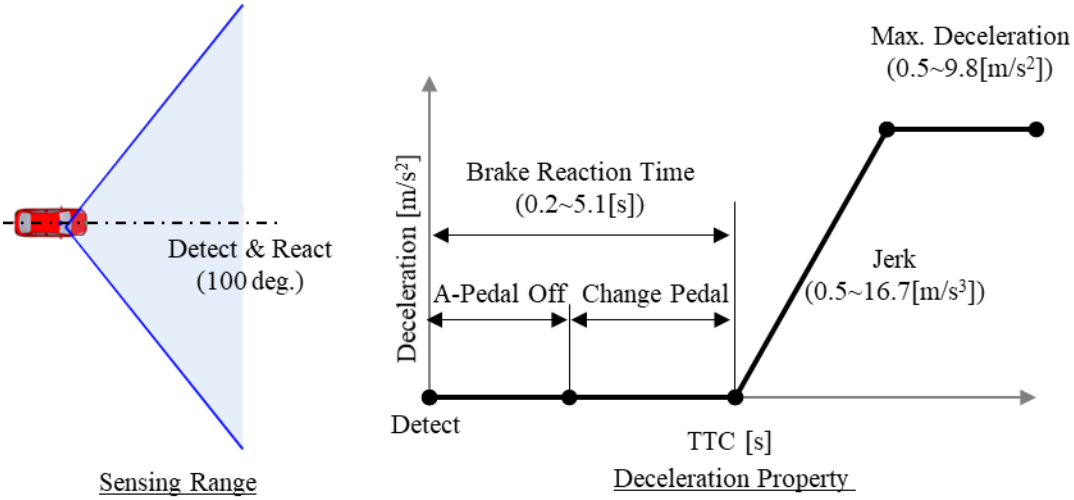

(b)Driver's braking model

Figure 3. Properties for AEB and driver's braking

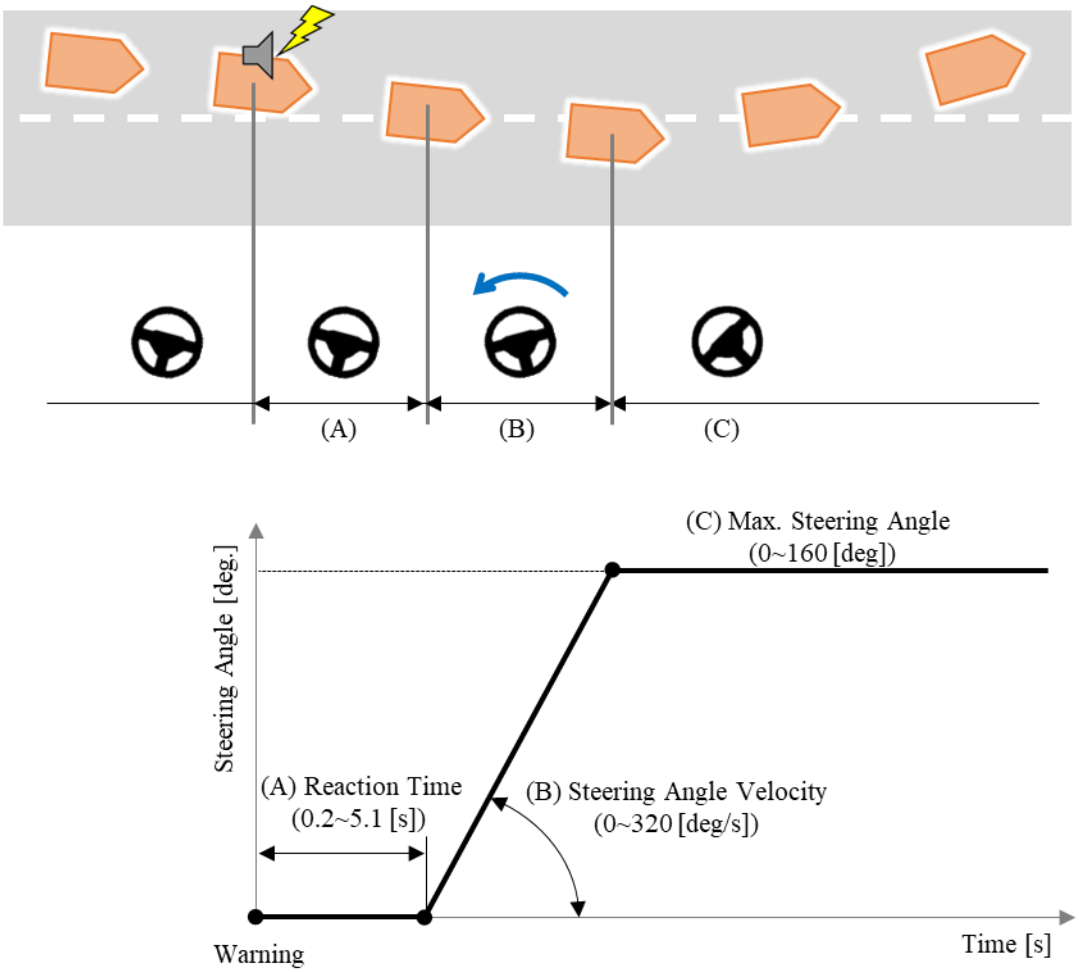

Figure 4. Property of driver steering to the center of the lane.

Crash Simulation

In the crash simulation, the fatal injury risk was estimated for the collision cases in the vehicle dynamics simulations. The virtual human body model THUMS (Total HUman Model for Safety) [14] was used to predict the fatal injury risk. The study focused on head injury as a representative form of fatal injury. The head injury criterion HIC_{15} was used to determine whether the injury level was fatal. First, crash simulations were conducted without AEB then the fatal injury risk was calculated. Next, crash simulations were conducted with AEB then the fatal injury risk was calculated again. The effectiveness of AEB was defined as the percentage of the reduction in the number of fatal injury cases by AEB. The benefit of AEB in injury mitigation was estimated by multiplying the fatality reduction rate by the percentage of the collision scenario in the total fatal collisions in Japan. The injury prediction method for pedestrians and occupants in the collision cases is described below. Figure 5 illustrates the flow of prediction process. First, crash simulations were conducted using THUMS and the vehicle model to construct a database indicating the relationship between the crash conditions and the HIC_{15} values. Using the database, a Reduced Order Model (ROM) was generated to calculate the injury value from the given crash conditions in a short time. A neural network was used to generate the ROM. The ROM calculated the injury values in tens of thousands of collision cases in a very short time. The conditions of a collision case were the input data to the ROM and the HIC_{15} value was the output. If the HIC_{15} value exceeded 700, it was regarded as a fatal collision case. LS-DYNA from ANSYS was used for the crash simulations. LS-OPT from ANSYS was used to generate the ROM and to calculate injury values.

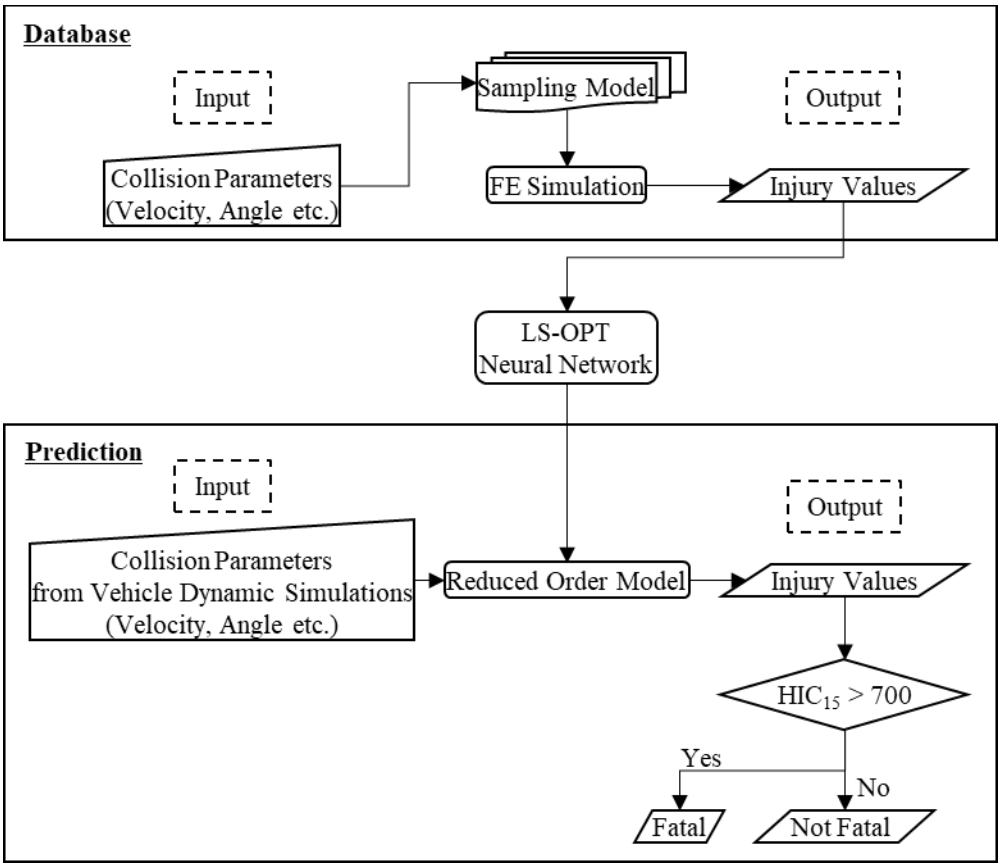

Figure 5. Flow of injury prediction process.

Crash Simulation Model THUMS AM50 Version 4.02 was used to represent the pedestrian or occupant in crash simulations. A midsize sedan was assumed as the subject vehicle (Figure 6). The collision conditions were changed parametrically by varying the numerical values. The parameter range of crash simulation covered all the collision cases in the vehicle dynamics simulation (Table 3). For pedestrian crossing, it was assumed that a pedestrian crossed the road in front of the vehicle then collided. The pedestrian collisions at the intersection occurred when the vehicle was turning right or left. The pedestrian posture was adjusted to comply with EuroNCAP TB024 [15]. The vehicle speed was varied from 10 to 60 kph, the collision angle was varied from 20 to 160 deg, and the collision position was varied from -700 to 700 mm in the vehicle width direction. A total of 225 crash simulations were performed. The bicycle collisions at the intersection occurred when the bicycle entered the intersection from the crossing road and collided with the vehicle's front. The other scenario was that the vehicle turned right or left at the intersection, and then collided with the bicycle. A city cycle was assumed. THUMS was placed on to the bicycle model. The vehicle speed varied from 10 to 60 kph, the bicycle speed varied from 3 to 23 kph, the collision angle varied from 0 to 180 deg, and the position varied from -650 to 1850 mm in the vehicle width direction. A total of 700 crash simulations were performed. The motorcycle collisions occurred when the motorcycle entered the intersection, and then collided with the vehicle front. A standard motorcycle was assumed. THUMS was placed on to the motorcycle model. The vehicle speed varied from 10 to 60 kph, the motorcycle speed varied from 10 to 60 kph, and the position varied from -440 to 1660 mm in the vehicle width direction. A total of 350 crash simulations were performed. The crash simulations were performed until the head contacted the vehicle and the head acceleration reached the maximum peak. It was assumed that pedestrians, bicyclists, and motorcyclists did not perform any avoidance or defensive actions before the collision.

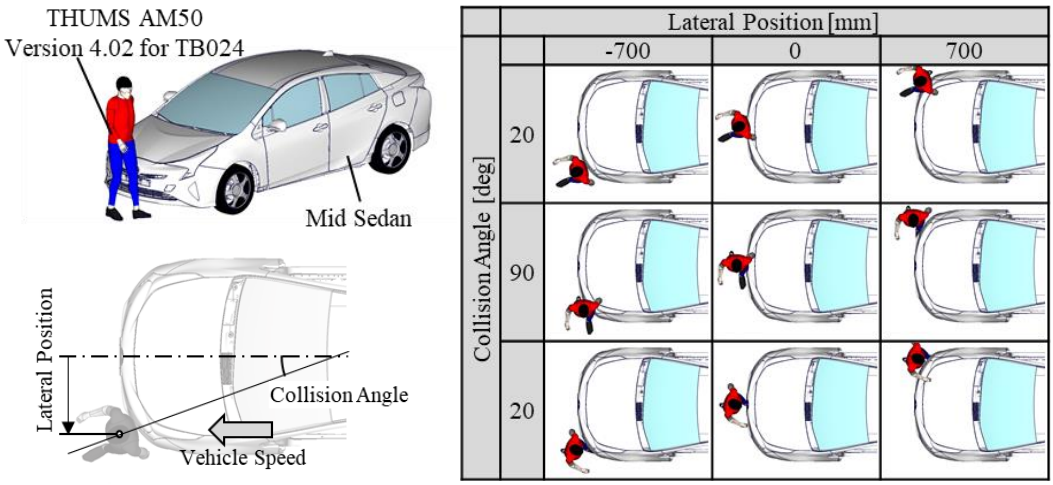

(a) Pedestrian (Scenario (i), (iv), (vi))

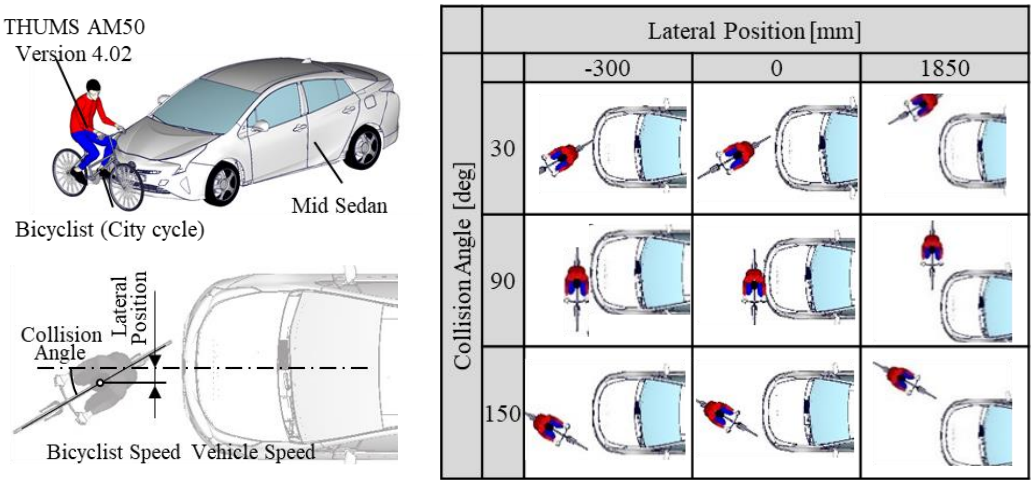

(b) Bicyclist (Scenario (ii), (v), (vii))

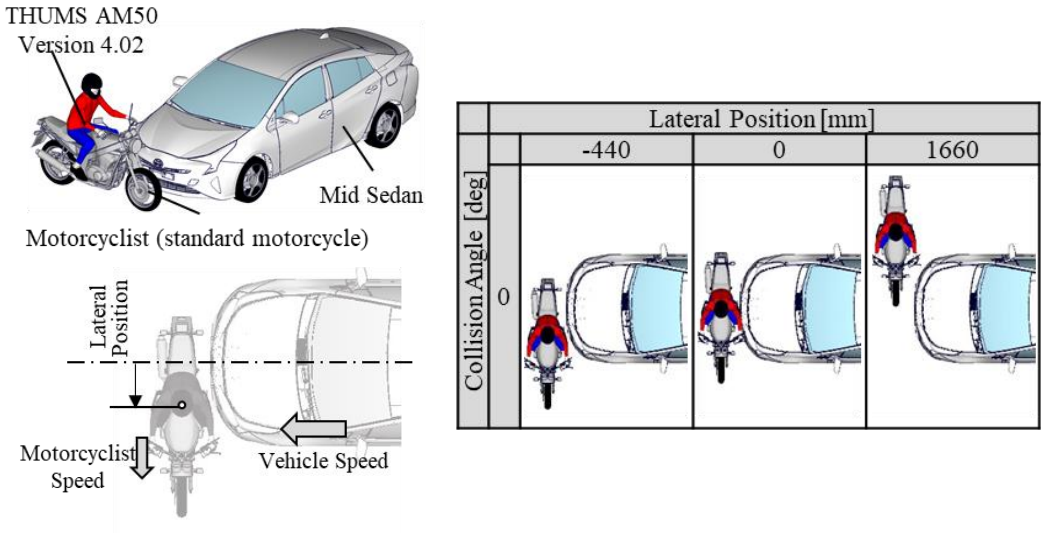

(c) Motorcyclist (Scenario (iii))

Figure 6. Crash simulation models.

Table 3.
Crash simulation parameters and ranges.

		Parameters				Number of Simulations
		Vehicle Speed	Bicyclist/Motorcyclist Speed	Collision Angle	Lateral Position	
Unit		kph	kph	deg	mm	
Range	Pedestrian	10 ~ 60	0	20 ~ 160	-700 ~ 700	225
	Bicyclist	10 ~ 60	3 ~ 23	0 ~ 180	-650 ~ 1850	700
	Motorcyclist	10 ~ 60	10 ~ 60	90	-440 ~ 1660	350

RESULT

Vehicle Dynamics Simulation

Collision Avoidance Effect of AEB and LDW A total of 153,000 cases were performed in the vehicle dynamics simulation, replicating the top nine collision scenarios in Japan. Without AEB or LDW, collision occurred in 117,031 out of 153,000 cases. With AEB or LDW, collision occurred in 48,030 cases. The reduction by AEB/LDW was calculated as 59.0 %. The benefit of AEB/LDW in collision avoidance was estimated as 29.9 % (Table 4). The contribution of AEB and LDW was 28.8 % and 1.1 %, respectively.

Table 4.
Benefit of AEB/LDW in collision avoidance.

No.	ADAS	Collision Scenario	Percentage of Collision in the Field	Number of Collision (ADAS inactivated)	Number of Collision (ADAS activated)	Collision Avoidance Effect	Benefit of AEB/LDW in Collision Avoidance
(i)	AEB	Pedestrian Crossing	6.2%	3,054	491	83.9 %	28.8%
(ii)		Bicyclist Crossing	24.5%	4,108	605	85.3 %	
(iii)		Motorcyclist Crossing		7,869	6,011	23.6 %	
(iv)		Pedestrian in Right-Turn	12.7%	17,000	4,265	74.9 %	
(v)		Bicyclist in Right-Turn		17,000	1,353	92.0 %	
(vi)		Pedestrian in Left-Turn		17,000	7,273	57.2 %	
(vii)		Bicyclist in Left-Turn		17,000	32	99.8 %	
(viii)	LDW	Single-Vehicle Collision	2.7%	17,000	13,390	21.2 %	1.1 %
(ix)		Head-on Collision with Vehicle	3.5%	17,000	14,610	14.1 %	
Total			-	117,031	48,030	59.0 %	29.9 %

<u>Pedestrian Crossing</u> In scenario (i), pedestrians crossing, collisions occurred in 3,054 out of 17,000 cases without AEB, while 491 cases were with AEB. The reduction of collision cases by AEB was 83.9 %. Figure 7 shows the time history curve of the vehicle speed for one of the non-collision cases with AEB (vehicle speed 54.2 kph, crossing angle 0 deg, pedestrian speed 1.3 kph). Figure 8 shows the vehicle behavior in the same case. Without AEB, the driver applied the brake at 0.6 seconds after recognizing the pedestrian who suddenly appeared. The 0.6 seconds corresponds to the time needed for the driver to make a decision and step on the brake pedal. In this case, the vehicle did not stop in front of the pedestrian. The vehicle speed was 41.9 kph at the time of collision. With AEB, the brake was activated immediately after the sensor detected the pedestrian. In that case, the vehicle stopped in front of the pedestrian. Figure 9 shows the frequency distribution of vehicle speed reduction in the 3,054 cases with and without AEB. The average speed reduction with AEB was 48.4 kph, which was 6.2 kph greater than that without AEB.

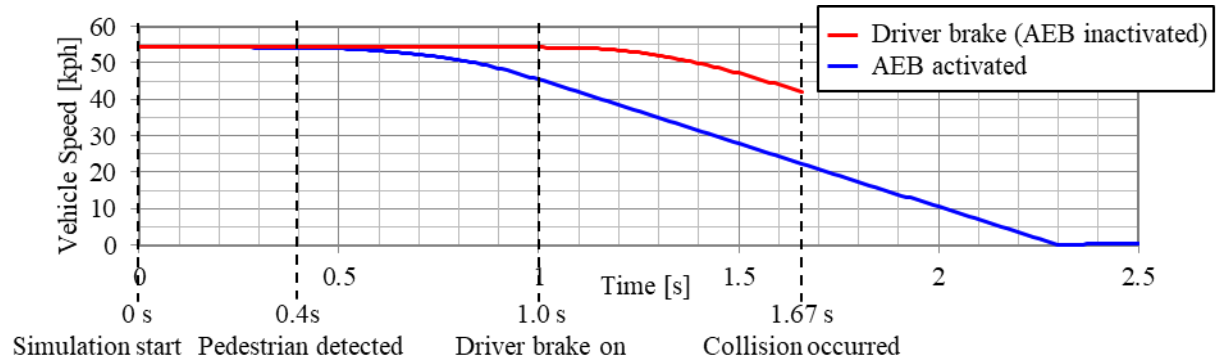

Figure 7. Time history curves of vehicle speed.

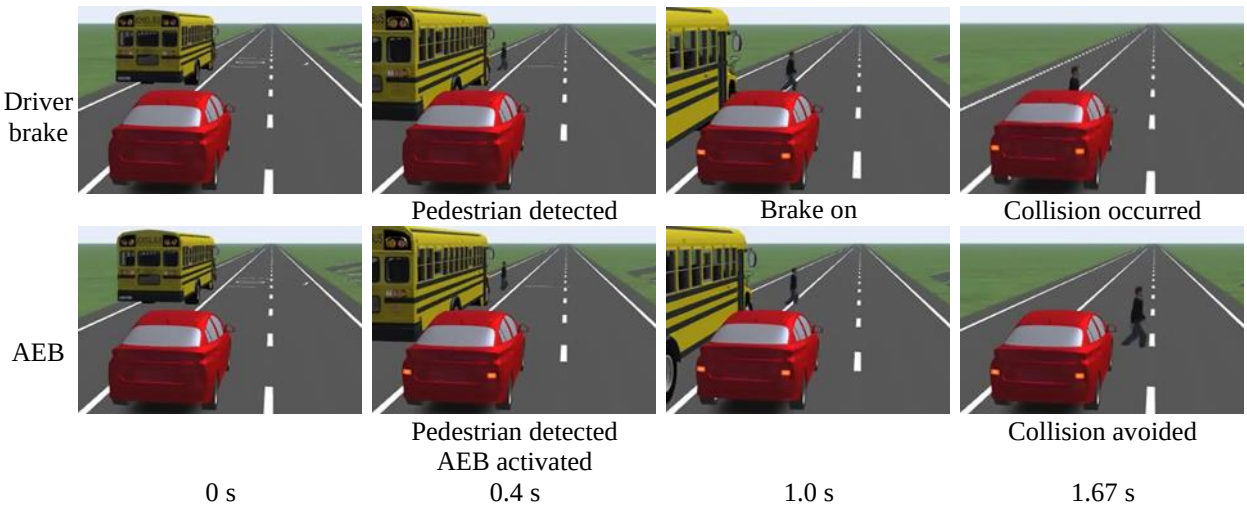

Figure 8. Vehicle behaviors.

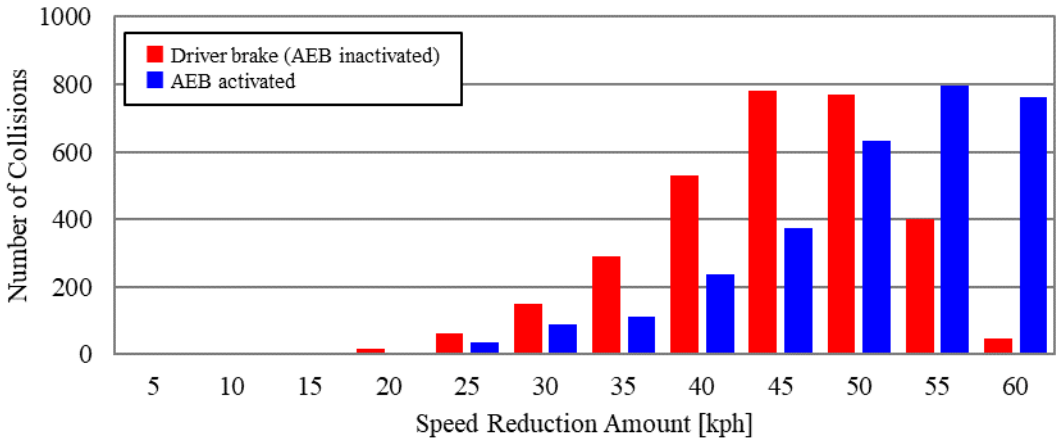

Figure 9. Frequency distribution of vehicle speed reduction.

Bicyclist/Motorcyclist Crossing In scenario (ii), bicyclist collision at the intersection, collisions occurred in 4,108 out of 17,000 cases without AEB, while 605 cases with AEB. The collision reduction rate by AEB was calculated as 85.3 %. In scenario (iii), motorcyclist collision at the intersection, collisions occurred in 7,869 out of 17,000 cases without AEB, while 6,011 cases with AEB. The collision reduction rate by AEB was calculated as 23.6 %. Figure 10 shows the time history curve of the vehicle speed in one of the non-collision cases with AEB (vehicle speed 59.9 kph, bicycle speed 15.3 kph). Figure 11 shows the vehicle behavior in the same case. Without AEB, the driver applied the brakes at 0.8 seconds after recognizing the bicycle suddenly appeared in the intersection. In this case, the vehicle did not stop in front of the bicycle. The vehicle speed was 39.8 kph at the time of collision. With AEB, the system activated the brake immediately after the sensor detected the bicycle. In that case, the vehicle stopped in front of the bicycle. Without AEB, collision occurred in 4,108 cases in scenario (ii), and 7,869 cases in scenario (iii). Figure 12 shows the frequency distribution of vehicle speed reduction in the collision cases with bicycle or motorcycle. In scenario (ii), the average speed reduction with AEB was 44.5 kph. It was greater than that without AEB by 6.8 km/h. In scenario (iii), the average speed reduction with AEB was 35.2 kph, which was 2.4 km/h greater than that without AEB.

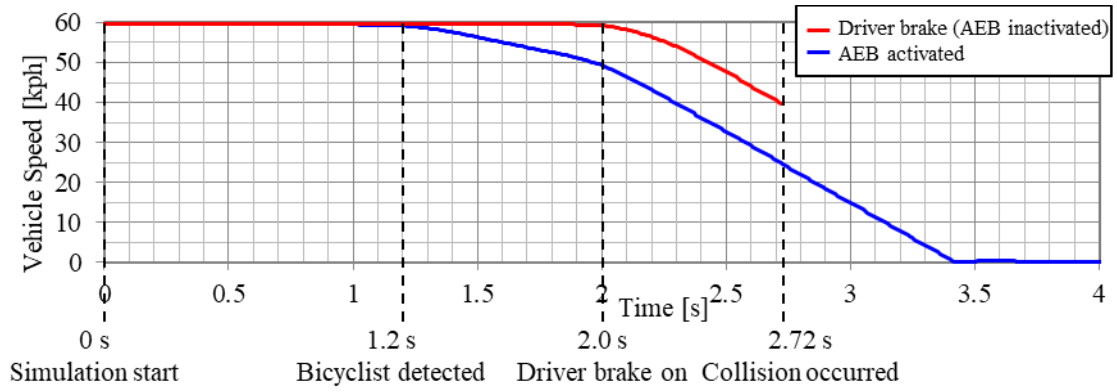

Figure 10. Time history curves of vehicle speed.

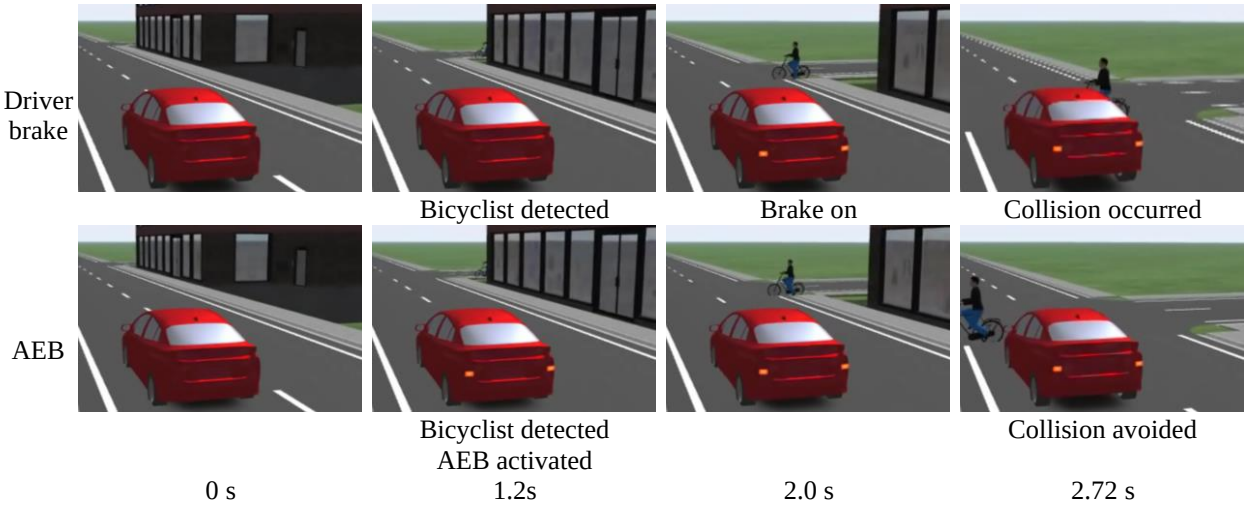

Figure 11. Vehicle behaviors.

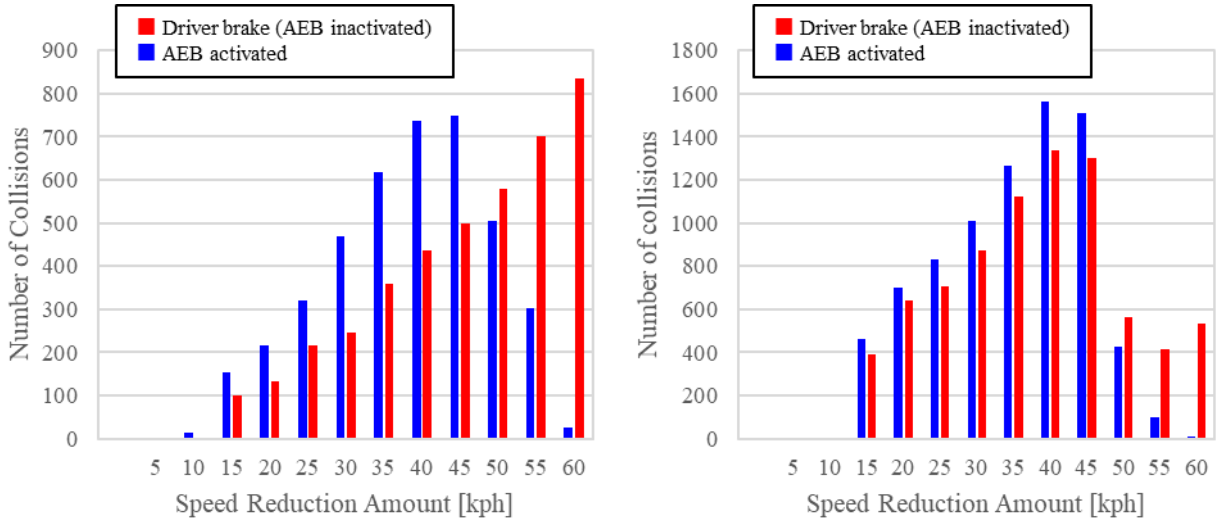

(a) Scenario(ii) Bicycle crossing *(b) Scenario(iii) Motorcycle crossing*

Figure 12. ***Frequency distribution of vehicle speed reduction.***

Pedestrian/Bicyclist in Turning In scenario (iv)-(vii), collisions with pedestrians and bicyclists when the vehicle is turning right or left at an intersection, it was assumed that the driver missed the pedestrian or the bicyclist and did not apply the brake. Without AEB, collisions occurred in all 17,000 cases. With AEB, collisions occurred in 4,265 out of 17,000 cases in scenario (iv), 1,353 cases in scenario (v), 7,273 cases in scenario (vi), and 32 cases in scenario (vii). The collision avoidance effect by AEB was 74.9 % in scenario (iv), 92.0 % in scenario (v), 57.2 % in scenario (vi), and 99.8 % in scenario (vii). Figure 13 shows the time history curve of the vehicle speed in one of the non-collision cases with AEB (scenario (iv), vehicle speed 19.6 kph, pedestrian speed 1.3 kph). Figure 14 shows the vehicle behavior in the same case. Without AEB, the vehicle continued turning right despite the presence of pedestrian. A collision occurred in this case. With AEB, the sensor detected the pedestrian during the right turn and the system stopped the vehicle in front of the pedestrian. Figure 15 shows the frequency distribution of the vehicle speed reduction in the collision cases with AEB. The average reduction in speed was 12.9 kph in scenario (iv), 16.2 kph in scenario (v), 15.9 kph in scenario (vi), and 15.3 kph in scenario (vii) with AEB activated. Table 5 compares the collision avoidance effects between the moving directions. When pedestrians or bicyclists moved in the same direction of the vehicle, the collision avoidance effects were 49.8 % in scenario (iv), 84.1 % in scenario (v), 19.2 % in scenario (vi), and 99.6 % in scenario (vii). When moving in the opposite direction of the vehicle, the collision avoidance effects were 100 % in scenario (iv), (v), and (vii) and 97.3 % in scenario (vi).

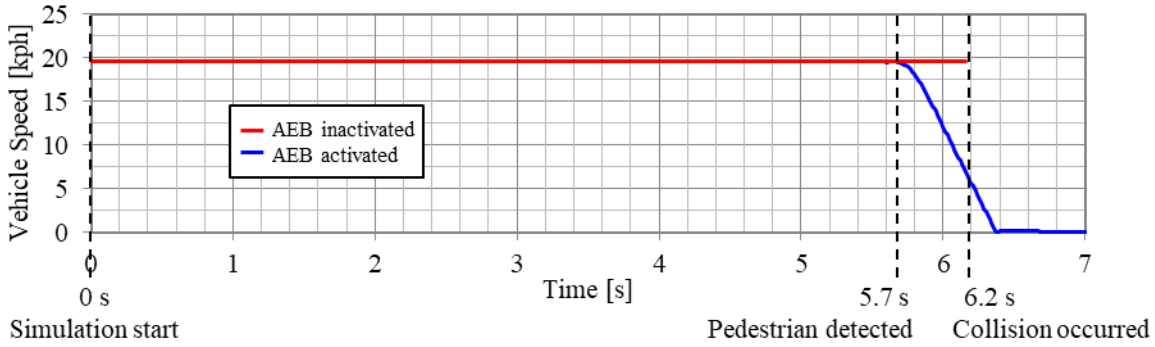

Figure 13. Time history curves of vehicle speed.

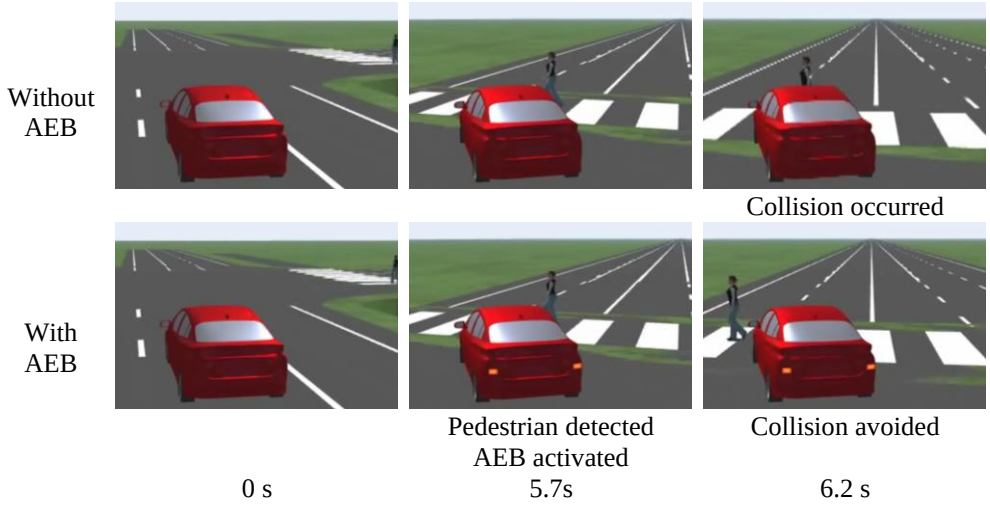

Figure 14. Vehicle behaviors.

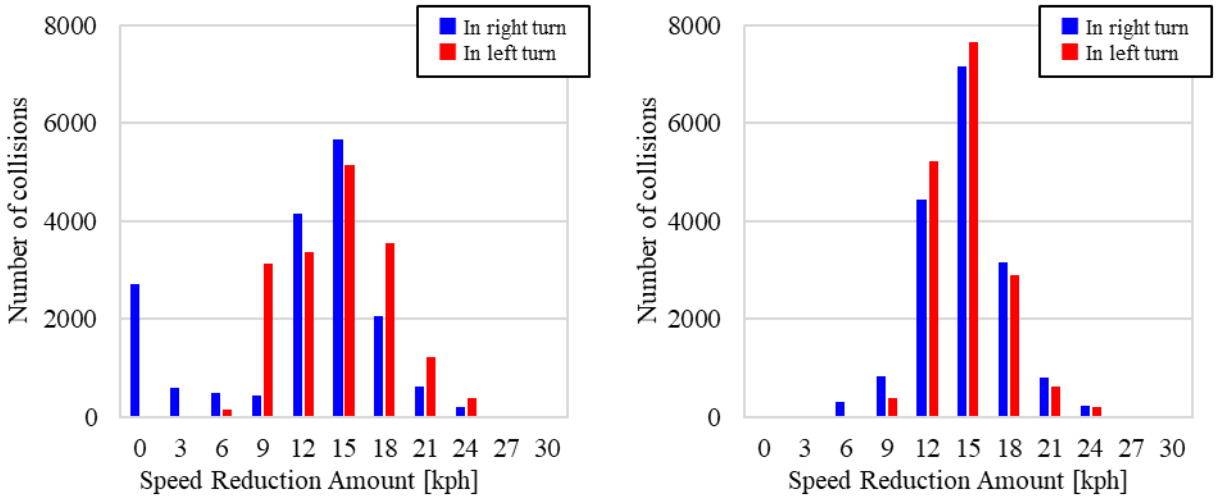

(a) Scenario(iv), (vi) Pedestrian in right/left turn *(b) Scenario(v), (vii): Biyclist in right/left turn*

Figure 15. Frequency distribution of vehicle speed reduction.

Table 5.
Reduction rates in collisions where the pedestrian/bicyclist coming from same/opposite direction while the vehicle is turning.

Scenario	ADAS	Collision Scenario	Direction	Number of Collision (ADAS inactivated)	Number of Collision (ADAS activated)	Collision Avoidance Effect
(iv)	AEB	Pedestrian in Right-Turn	Same	8,500	4,265	49.8 %
			Opposite	8,500	0	100 %
(v)		Bicyclist in Right-Turn	Same	8,500	1,353	84.1 %
			Opposite	8,500	0	100 %
(vi)		Pedestrian in Left-Turn	Same	8,500	7,051	19.2 %
			Opposite	8,500	222	97.3 %
(vii)		Bicyclist in Left-Turn	Same	8,500	32	99.6 %
			Opposite	8,500	0	100 %

Lane Departure In scenario (viii), (ix), lane departure and collision with a fixed obstacle (single vehicle collision) or an oncoming vehicle (head-on collision), it was assumed that the driver did not control the steering without recognizing the risk. Without LDW, collisions occurred in all 17,000 cases. With LDW, collisions occurred in 13,390 out of the 17,000 cases in scenario (viii) and 14,610 cases in scenario (ix). The collision avoidance effect by LDW was 21.2 % for single vehicle collisions and 14.1 % for head-on collisions. Figure 16 shows the time history curve of the steering angle in one of the non-collision cases with LDW (scenario (viii), vehicle speed 56.6 kph, curve radius 450 m). Figure 17 shows the vehicle behavior in the same case. Without LDW, the vehicle deviates from the lane and collided with the guardrail. With LDW, the driver controlled the steering at 0.7 s after the warning. The delay time represented the driver's reaction time. The vehicle returned to the lane before colliding with the guardrail. Figure 19 shows the relationship between collision avoidance effect and vehicle departure speed/angle. The collision avoidance effect ranged from 10 to 30 % for all speed ranges. As for the departure angle, the collision avoidance effect

ranged from 26 to 50 % when the angle was less than 5 degrees. The collision avoidance effect was lower than 14 % when the angle was 5 degrees or greater.

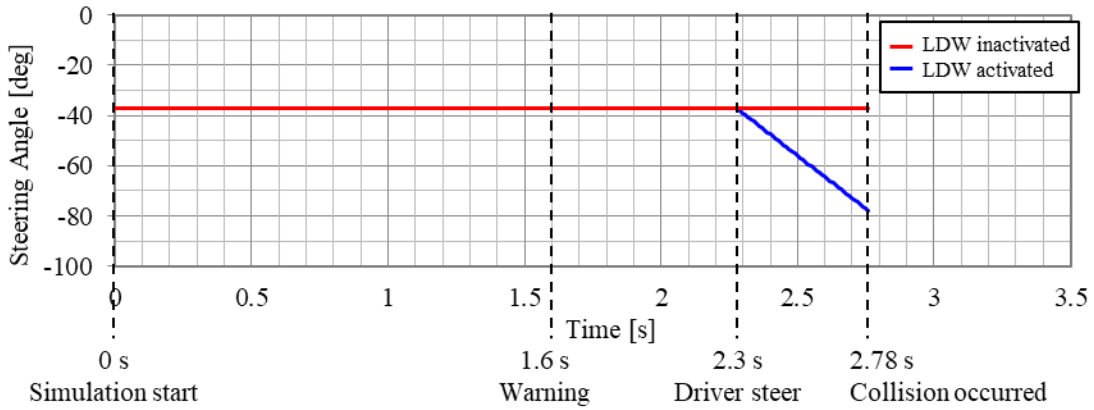

Figure 16. Time history curves of steering angle.

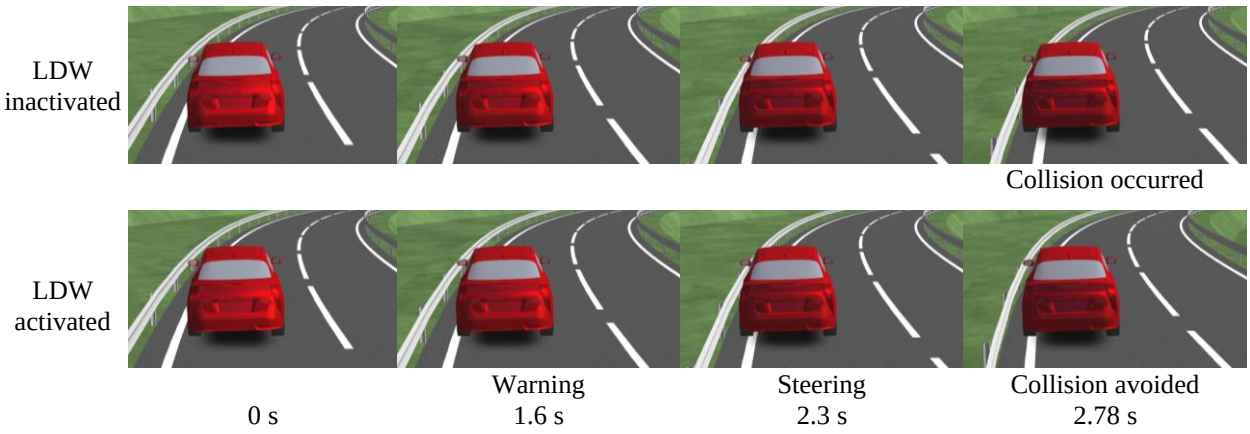

Figure 17. Vehicle behaviors.

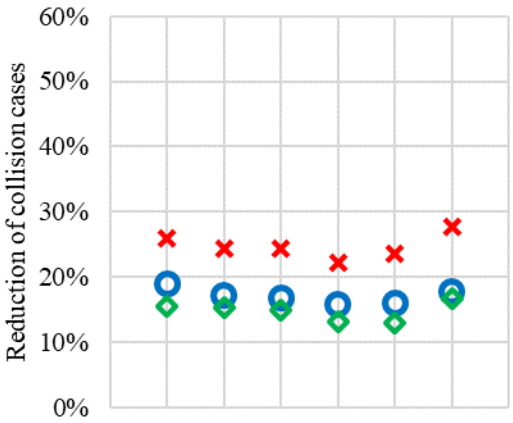

Relationship between collision avoidance effect and vehicle departure speed

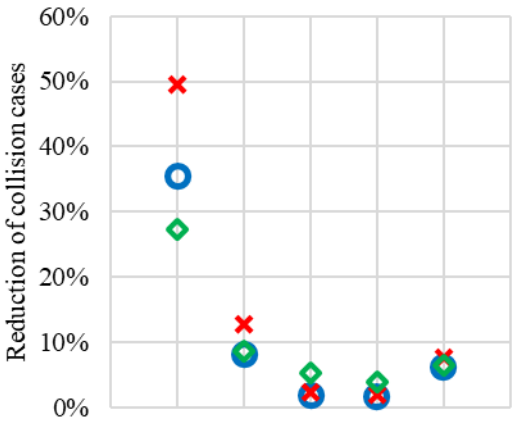

Relationship between collision avoidance effect and vehicle departure angle

Figure 18. Reduction of collision cases.

Crash Simulations

Kinematics and Head Impact Response Crash simulations were conducted using THUMS and the vehicle model in order to generate a ROM for rapid injury prediction. The paper focuses on the case where the vehicle speed was 60 kph, the collision angle was 90deg, and the head contact position was 600 mm from the vehicle center in the width direction. Figure 19 shows the whole-body behavior of the pedestrian during the collision. Figure 20 shows the time history curve of the head acceleration. The upper body rotated after the lower limbs contacted the bumper and the pelvis contacted the hood. The shoulder contacted the rear end of the hood. Approximately 110 ms after the start of the collision, the head contacted the A-pillar. The head displacement was 40 mm in the vehicle width direction. The head acceleration reached the maximum peak (241 G) when contacting with the A-pillar. The HIC_{15} value was calculated as 1,522. Figure 21 shows the whole-body behavior of the bicyclist traveling at 23 kph. Figure 22 shows the time history curve of the head acceleration. Initially, the lower limbs contacted the bumper. The upper body rotated after the pelvis contacted the hood. Then, the shoulder contacted the windshield glass (W/S). Approximately 130 ms after the start of the collision, the head contacted the roof. The head displacement was 730 mm in the vehicle width direction. The head acceleration reached the maximum peak (94G) at the timing when contacting the roof. The HIC_{15} value was calculated as 640. Figure 23 shows the whole-body behavior of the motorcyclist when colliding with the vehicle traveling at a speed of 40 kph. Figure 24 shows the time history curve of the head acceleration. Initially, the lower limbs and the motorcycle body contacted the vehicle front, and the hood was deformed. The upper body rotated after the pelvis contacted the hood. After that, the shoulder contacted the W/S. The head contacted the A-pillar at about 140 ms from the start of the collision. The head displacement was 1,285 mm in the vehicle width direction. The head acceleration reached the maximum peak (188 G) at the timing when contacting the A-pillar. The HIC_{15} value was calculated as 1,573.

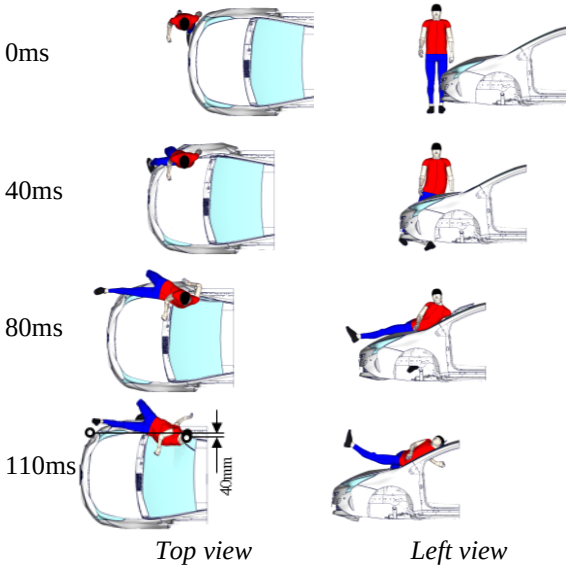

Figure 19. Whole-body behavior.

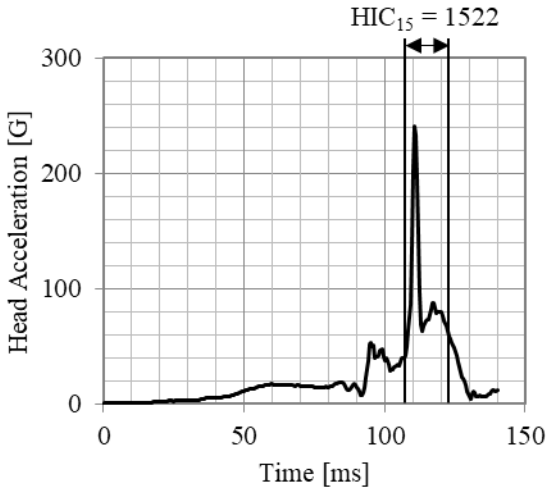

Figure 20. Time history curve of acceleration of pedestrian's head.

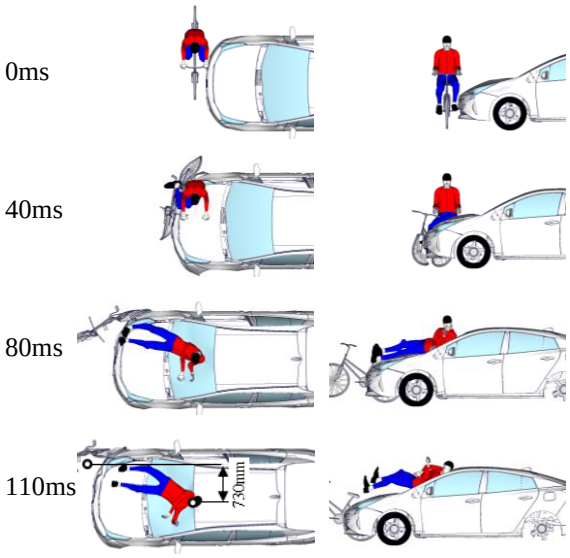

Figure 21. Whole-body behavior. (Bicycle speed = 23 kph)

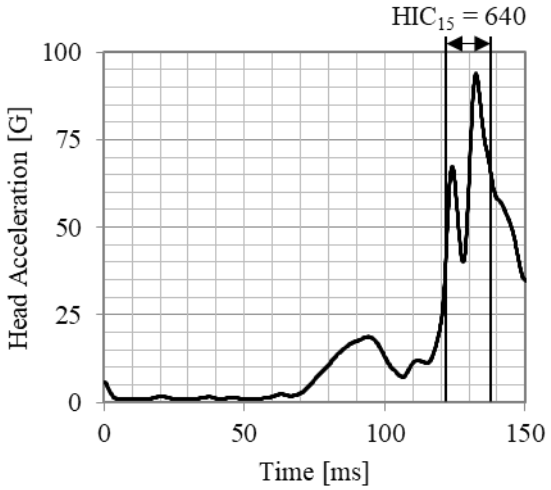

Figure 22. Time history curve of acceleration of bicyclist's head.

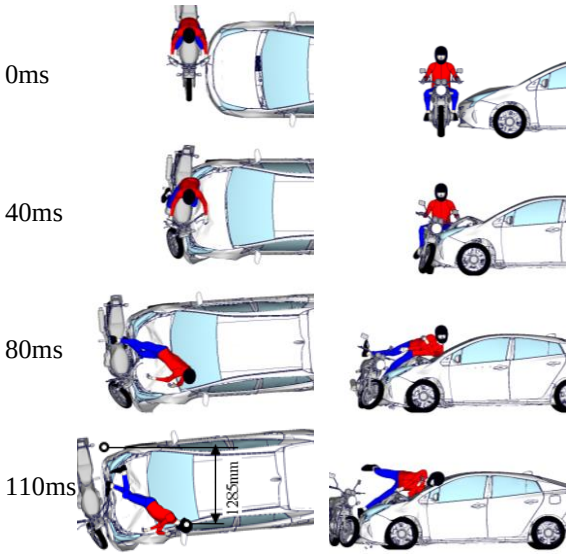

Figure 23. Whole-body behavior. (Motorcycle speed = 40 kph)

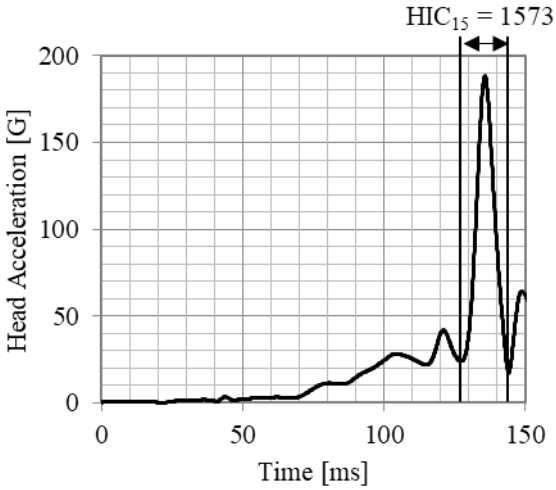

Figure 24. Time history curve of acceleration of motorcyclist's head.

Head Impact Conditions Figure 25 shows the distribution of HIC_{15} (over 700/not over 700) for the pedestrians, bicyclists, and motorcyclists in relation to the head contact points on the vehicle. In the pedestrian cases, the head contact points distributed above the W/S. The points with the HIC_{15} values over 700 were found near the A pillar. In the bicyclist cases, the head contact points distributed on the hood, W/S, and roof. The points with the HIC_{15} values over 700 appeared near the A-pillar and the roof header. In the motorcyclist cases, the head contact points distributed from the hood to the W/S. The points with the HIC_{15} values over 700 were mostly observed near the A pillar.

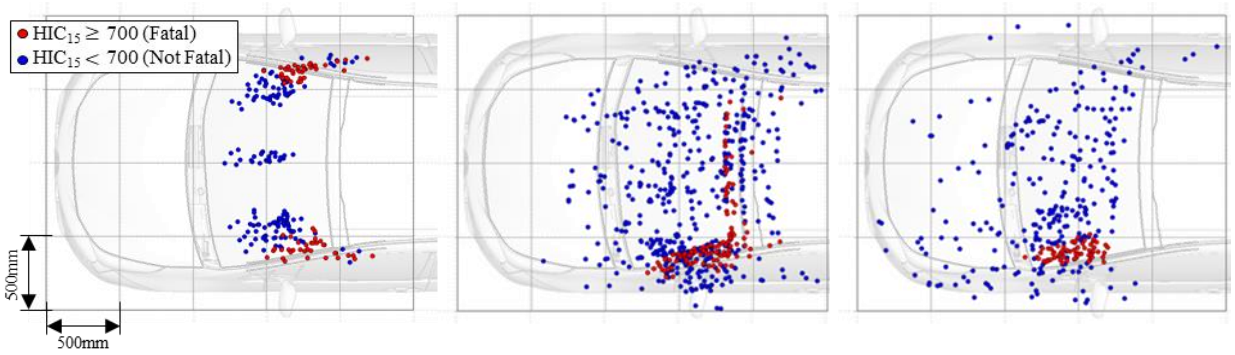

(a) Pedestrian *(b) Bicyclist* *(c) Motorcyclist*

Figure 25. Distributions of HIC_{15} value.

Reduced Order Model The collision parameters and the resultant HIC_{15} values were stored in the database. A ROM was generated to predict HIC_{15} values from the given collision conditions. A neural network was used to generate the ROM. The prediction accuracy of the generated ROM was verified by the leave-one-out cross-validation test. Figure 26 shows the validation results. The vertical axis is the predicted value by the ROM, and the horizontal axis is the HIC_{15} (true value) calculated by THUMS. The area under the curve (AUC) of the receiver operating characteristic (ROC) curve, a binary classification, was used as the evaluation index [16]. The ROMs generated for pedestrians, bicyclists, and motorcyclists were validated through the validation process described above. The AUC values were about 0.9 for all cases. Based on the results, it was confirmed that the generated ROMs had sufficient prediction accuracy.

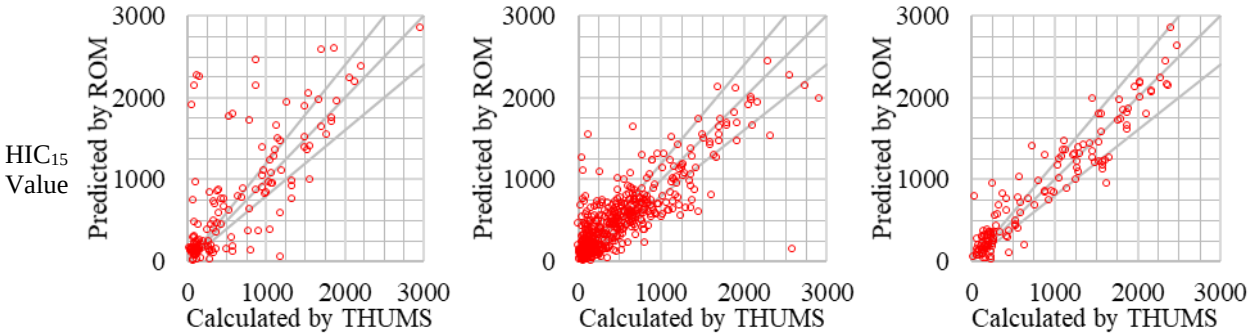

AUC 0.89 0.93 0.99

(a) Pedestrian *(b) Bicyclist* *(c) Motorcyclist*

Figure 26. Validations HIC_{15} value.

Injury Mitigation Effect of AEB The HIC_{15} values were predicted by ROM for the collision cases in vehicle dynamics simulations. Without AEB, fatal injuries were predicted in 415 out of 117,031 cases. With AEB, fatal injuries were predicted in 76 out of 48,030 cases. Based on these numbers, the injury mitigation effect of AEB was estimated to be 81.7 %. The benefit of AEB in injury mitigation in Japan, was estimated as 52.5 % (Table 6)

Table 6.
Benefit of AEB in injury mitigation.

No.	ADAS	Collision Scenario	Percentage of Fatalities in the Field	Number of Fatalities (ADAS inactivated)	Number of Fatalities (ADAS activated)	Injury Mitigation Effect	Benefit of AEB in Injury Mitigation
(i)	AEB	Pedestrian Crossing	40.2 %	123	5	95.9 %	52.5 %
(ii)		Bicyclist Crossing	6.7 %	142	0	100 %	
(iii)		Motorcyclist Crossing	3.9 %	122	71	42.0 %	
(iv)		Pedestrian in Right-Turn	1.9 %	10	0	100 %	
(v)		Bicyclist in Right-Turn		0	0	100 %	
(vi)		Pedestrian in Left-Turn	1.0 %	18	0	100 %	
(vii)		Bicyclist in Left-Turn		0	0	100 %	
(viii)	LDW	Single-Vehicle Collision	-	-	-	-	-
(ix)		Head-on Collision with Vehicle	-	-	-	-	
Total			-	415	76	81.7 %	52.5 %

<u>Pedestrian Crossing</u> Without AEB in scenario (i) of pedestrian crossing, fatal injuries were predicted in 123 out of 3,054 cases. With AEB, fatal injuries were predicted in 5 out of 491 cases. Based on these numbers, the injury mitigation effect by AEB was estimated as 95.9 %. Figure 27 shows the distribution of HIC_{15} (over 700/under 700) predicted by ROM in relation to the head contact point on the vehicle. The contact points were distributed from the A-pillar to the W/S. The points with the HIC_{15} values over 700 appeared near the A pillar.

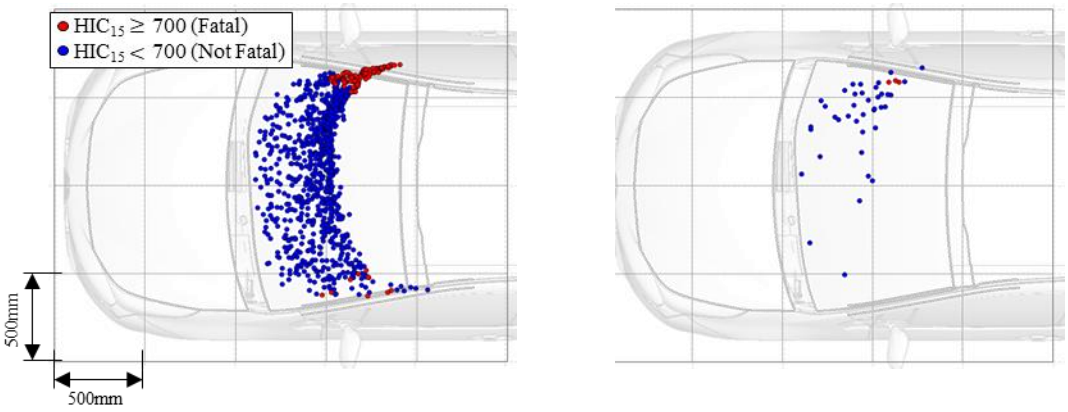

(a) Driver brake (without AEB) *(b) With AEB*

Figure 27. Distribution of HIC_{15} value.

Bicyclist/Motorcyclist Crossing Without AEB in scenario (ii) of bicycle collision at the intersection, fatal injuries were predicted in 142 out of 4,108 cases. With AEB, fatal injuries were not predicted. Based on these numbers, the injury mitigation effect by AEB was estimated as 100 %. Figure 28 shows the distribution of HIC_{15} values (over 700/under 700) predicted by ROM in relation to the head contact points on the vehicle. The contact points distributed from the hood, W/S, and roof header. The contact points with the HIC_{15} values over 700 mostly appeared near the A pillar and roof header. With AEB, the head did not contact the A-pillar or roof header. Without AEB in scenario (iii) of motorcycle collision at the intersection, fatal injuries were predicted in 122 out of 7,869 cases. With AEB, fatal injuries were predicted in 71 out of 6,011 cases. Based on these numbers, the injury mitigation effect by the AEB was estimated to be 42.0 %. Figure 29 shows the distribution of the HIC_{15} values (over 700/under 700) predicted by ROM in relation to the head contact points on the vehicle. The head contact points distributed from the hood to the W/S. The points with the HIC_{15} values over 700 appeared near the A pillar.

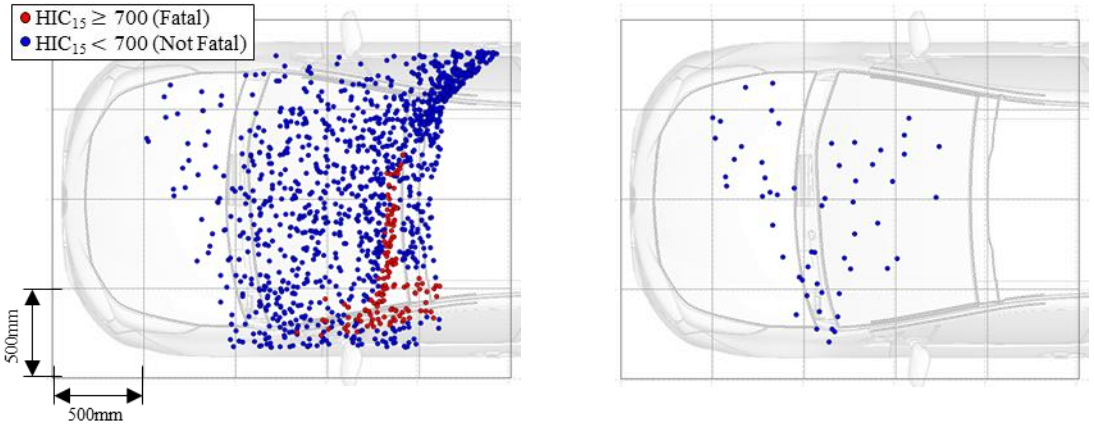

(a) Driver brake (without AEB) *(b) With AEB*

Figure 28. Distribution of HIC_{15} value. (Scenario (ii): Bicyclist)

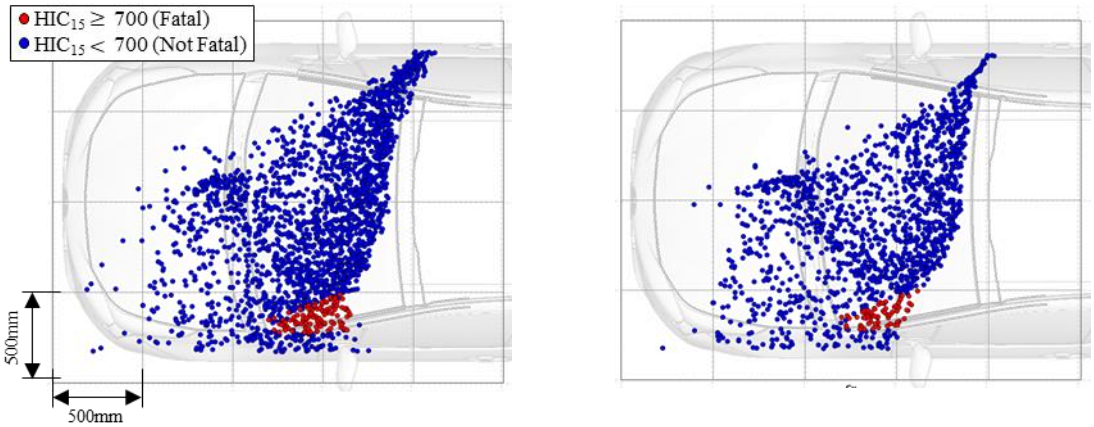

(a) Driver brake (without AEB) *(b) With AEB*

Figure 29. Distribution of HIC_{15} value. (Scenario (iii): Motorcyclist)

Pedestrian/Bicyclist in Turning In scenario (iv) and (vi), pedestrian collision in turning right/left at the intersection without AEB, fatal injuries were predicted in 10 out of 17,000 cases in the right-turn scenarios (iv) and 18 out of 17,000 cases in the left-turn scenarios (vi). With AEB, fatal injuries were not predicted. Figures 30 and 31 show the distribution of the HIC_{15} values (over 700/under 700) predicted by ROM in relation to the head contact points on the vehicle. The head contact points distributed from the A pillar to W/S. The points with the HIC_{15} values over 700 mostly appeared near the A pillar. In scenario (v) and (vii), bicyclist collision in turning right/left at the intersection

without AEB, fatal injuries were not predicted. Figures 32 and 33 show the distribution of the HIC_{15} values (over 700/under 700) predicted by ROM in relation to the head contact points on the vehicle. Without AEB, the head contact points distributed from the hood and W/S. With AEB the bicyclist head did not contact the vehicle.

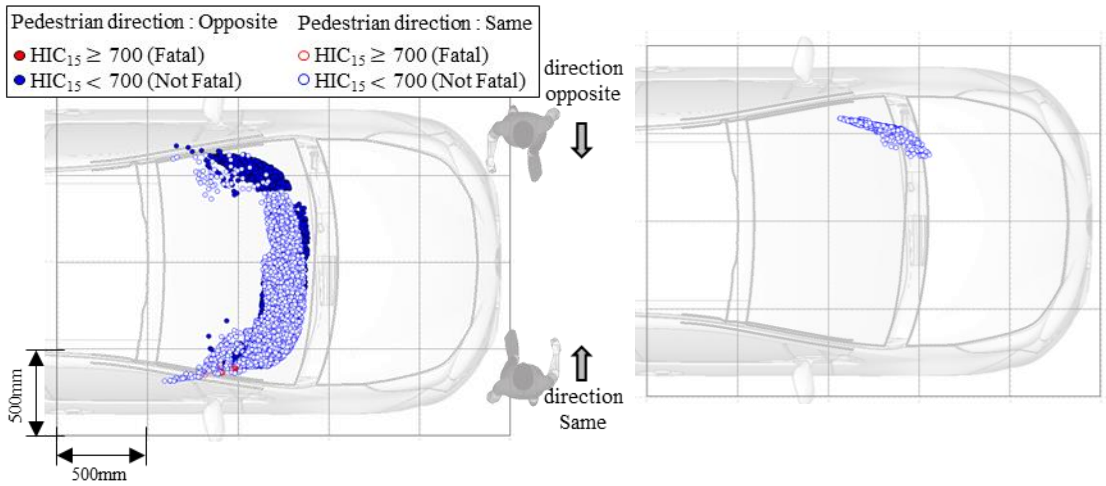

(a) Without AEB *(b) With AEB*

Figure 30. Distribution of HIC_{15} value. (Scenario (iv): Pedestrian in right turn)

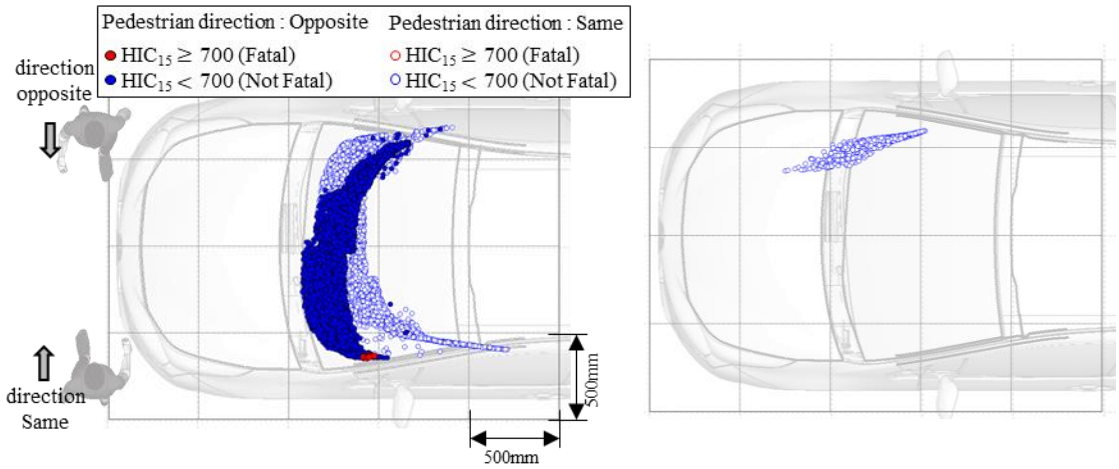

(a) Without AEB *(b) With AEB*

Figure 31. Distribution of HIC_{15} value. (Scenario (vi): Pedestrian in left turn)

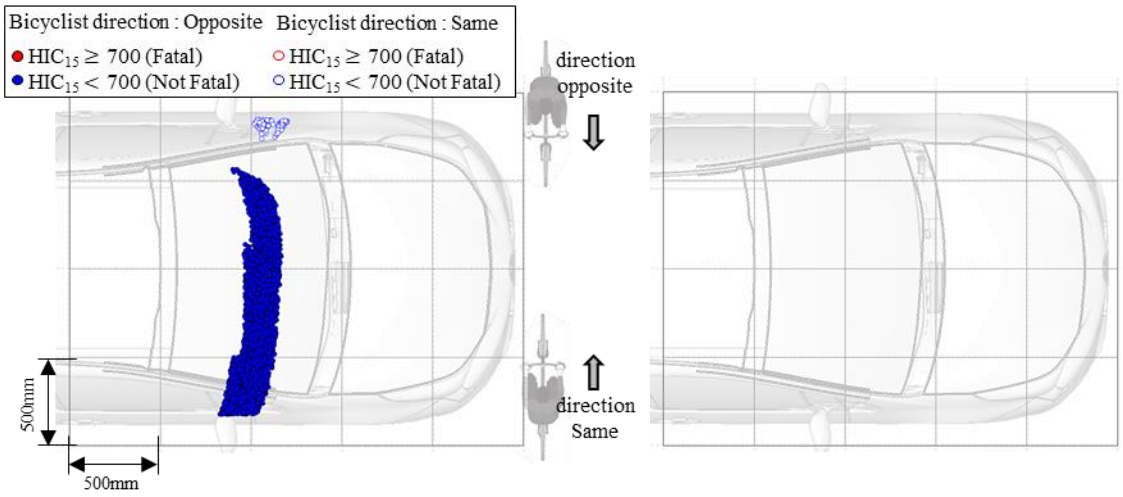

(a) Without AEB *(b) With AEB*

Figure 32. Distribution of HIC_{15} value. (Scenario (v): Bicyclist in right turn)

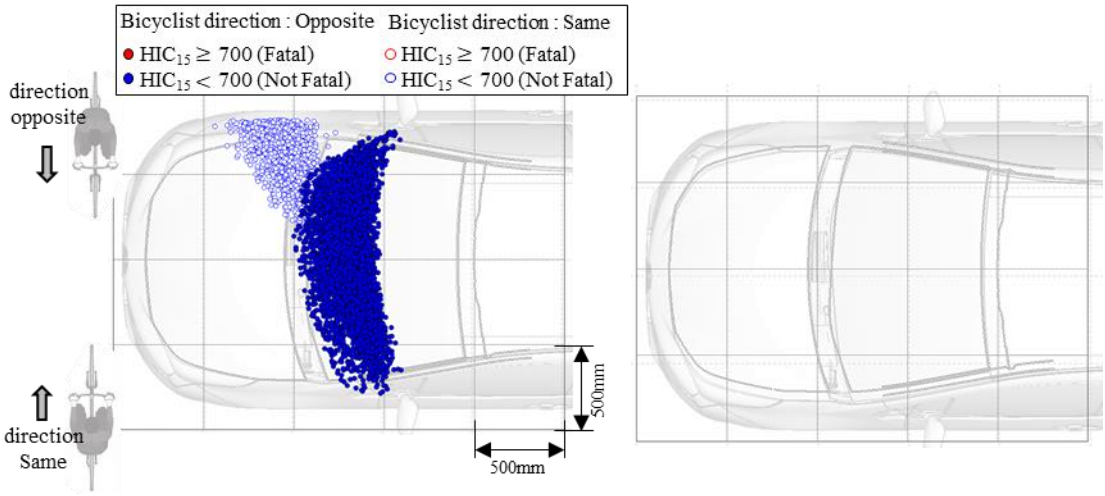

(a) Without AEB *(b) With AEB*

Figure 33. Distribution of HIC15 value. (Scenario (vii): Bicyclist in left turn)

DISCUSSION

The effectiveness of AEB/LDW was analyzed for the nine scenarios assumed in this study. In scenario (i) of pedestrian crossing, the collisions were avoided by the AEB in many cases and the number of fatal injuries was lower than the cases without AEB where the driver applied brake. Comparing the results of scenario (ii) and (iii), collisions with bicyclist and motorcyclist at the intersection, the collision avoidance effect by AEB was higher in the bicyclist cases than in the motorcyclist cases. In scenario (iv)-(vii), collisions with pedestrians and bicyclist while the vehicle was turning right or left at the intersection, the collision avoidance effect was higher when the pedestrian or bicyclist moved in the opposite direction of the vehicle than when they moved in the same direction. In scenario (viii) and (ix) of lane departure, the collision avoidance effect by LDW was higher in the cases against a fixed obstacle than those colliding with an oncoming car.

Pedestrian Crossing

In scenario (i) of pedestrian crossing, the collision avoidance effect by AEB was estimated to be 83.9 % and the injury mitigation effect was estimated to be 95.9 %. The study assumed the situation that a pedestrian appeared from the

blind spots of a parked vehicle. There was no significant difference in TTC at detection between AEB and the human driver (Figure 34). With AEB, the average stopping distance was shorter than that without AEB (human driver) by 4.9 m. The reduction in stopping distance contributed to the collision avoidance (Figure 35). In collision cases with AEB, the average collision speed was lower than that without AEB by 6.7 kph. The reduction in collision speed contributed to injury mitigation (Figure 36).

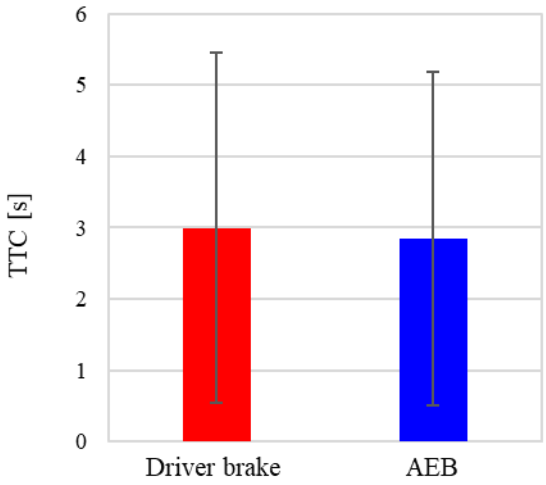

Figure 34. TTC by driver's braking and AEB.

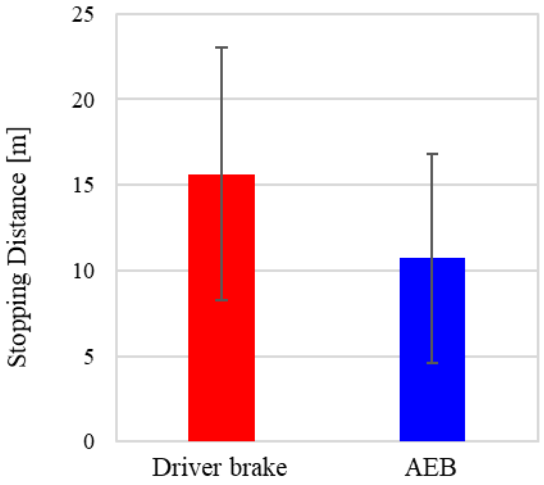

Figure 35. Stopping distance by driver's braking and AEB.

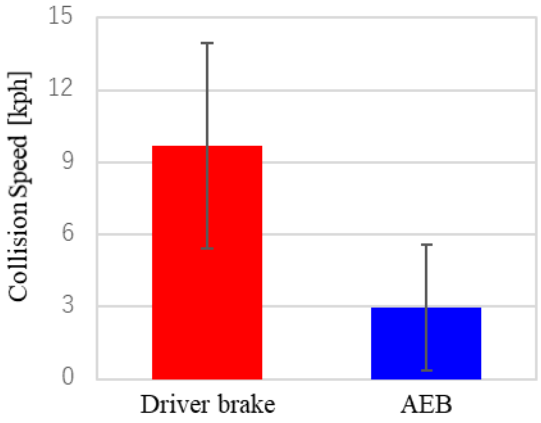

Figure 36. Collision speed.

Bicyclist/Motorcyclist Crossing

In scenarios (ii) and (iii), collisions with bicyclist and motorcyclist at the intersection, the collision avoidance effect by AEB was higher for bicyclist than for motorcyclist. Without AEB, the reduction in vehicle speed was 9.3 km/h greater (on an average) in collisions with bicyclist than those with motorcyclist. The speed of bicyclist was lower than the motorcyclist. The TTC values at detection were generally longer for bicyclists than those of motorcyclist. The longer TTC contributed to the collision avoidance (Figure 37).

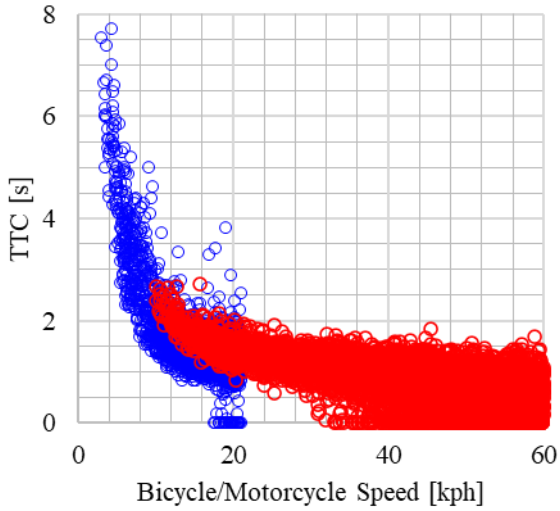

Figure 37. Distribution of TTC.

Pedestrian/Bicyclist in Turning

In scenario (iv)-(vii), collisions with pedestrians or bicyclists during right or left turn at the intersection, the collision avoidance effect when the pedestrian or bicyclist moved in the opposite direction of the vehicle was higher than that in the same direction. The pedestrians approaching from the opposite direction were detected early as they entered the field of view. Pedestrians moving in the same direction were not detected early as they stayed diagonally behind the vehicle in the sensor's blind spot for a long time (Figure 38).

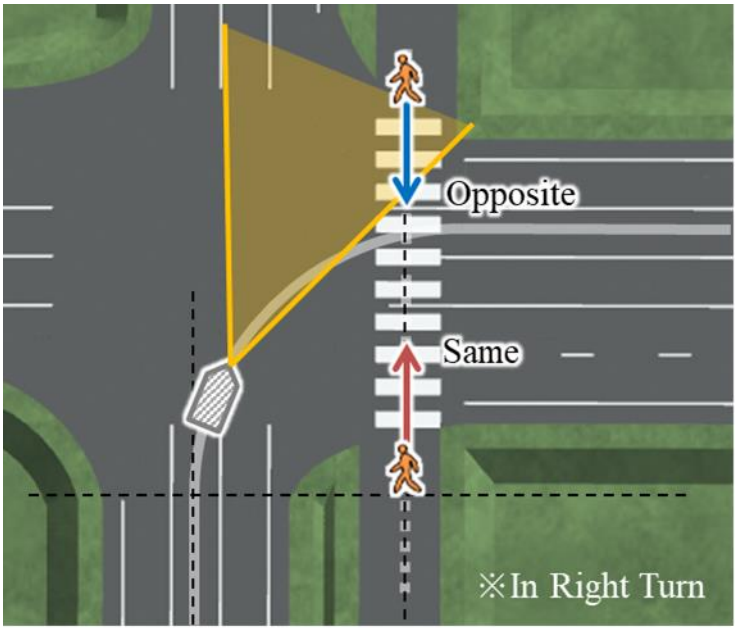

Figure 38. Field of view of a turning vehicle.

Lane Departure

In scenario (viii) and (ix) of lane departure, the collision avoidance effect by LDW was higher in the cases colliding with a fixed obstacle than those with an oncoming car. The collision avoidance effect decreased with the increase of deviation angle (Figure 18). For deviation angles of less than 5 degrees, the collision avoidance effect in the cases colliding with poles was higher than that with the guardrail or oncoming vehicles. The guardrail was a continuous structure along the road and could be a large obstacle for the vehicle. On the other hand, the pole was located at a specific position of the roadside. At the same deviation angle, collision with the guardrail could occur earlier than that

with the pole. This tendency appeared remarkably at small departure angles. The oncoming vehicle approached with speed and the time to avoid the collision was shortened. The time to the collision from the alert was longer in the cases with the pole and contributed to the higher collision avoidance effect (Figure 39).

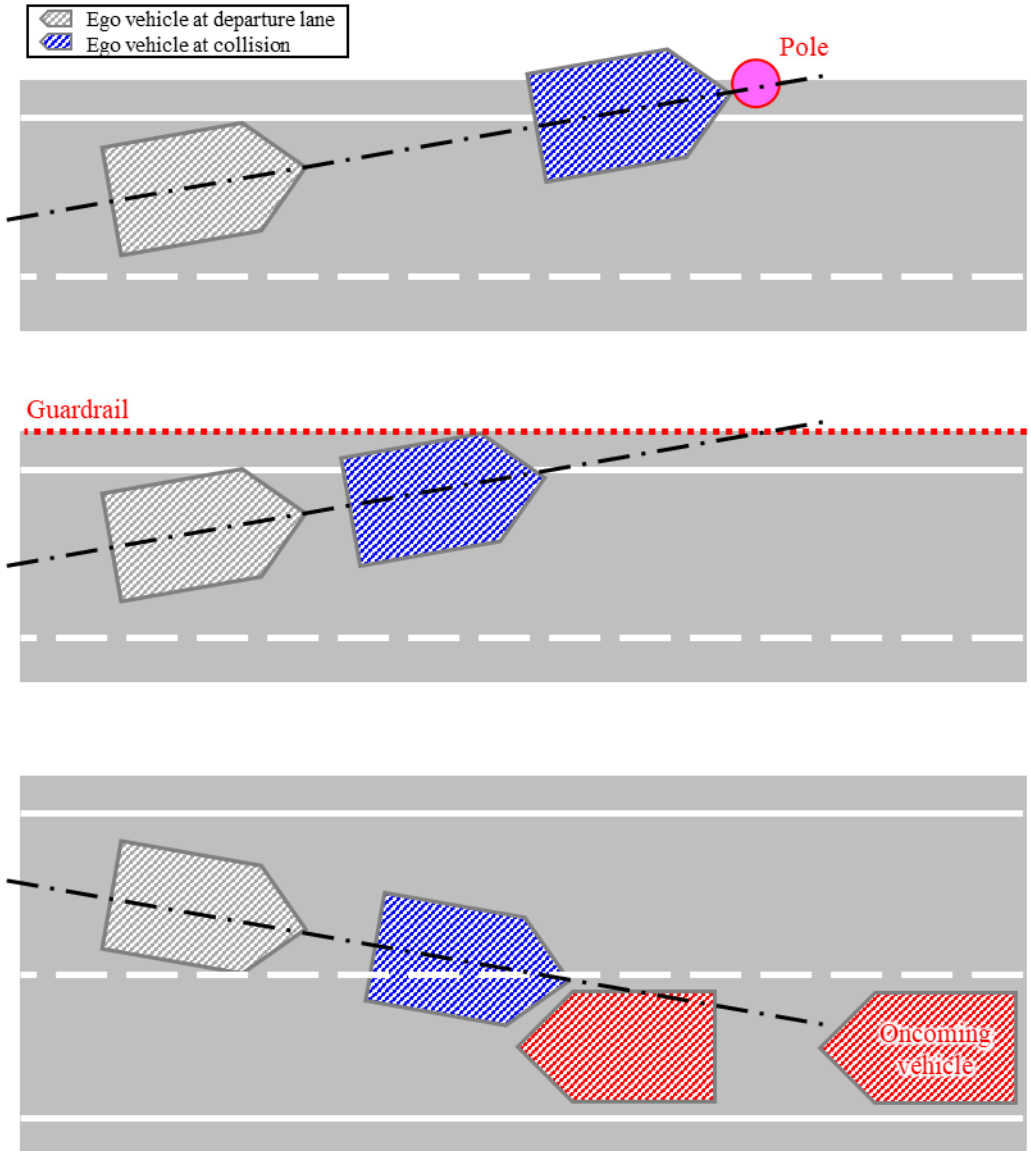

Figure 39. Behaviors of a vehicle deviates from its lane.

LIMITATION

In this study, the effectiveness of AEB/LDW were estimated through the vehicle dynamic simulations and crash simulations. The parameters of simulations varied to widely cover possible situations in the field. However, it did not perfectly cover all actual collision cases. In the simulation model, the sensor properly detected the obstacles and the system immediately activated AEB or LDW at the maximum performance. The real traffic environment has a wide range of variety in brightness, visibility and road surface conditions etc. There were other assumptions such as a midsize sedan for the vehicle type and a midsize adult male person for the occupant. The study used the head injury criterion for the judgement of fatal injury. In collisions with VRU, only collisions with vehicles were counted in the study while there were also road surface collisions in the field. Thus, actual collisions may have much more variety than the range assumed in this study. It is important to consider actual accident data to verify the accuracy of this

method for benefit estimation, and to consider the variation and diversity of factors that have a large impact on prediction accuracy.

CONCLUSION

In this study, a simulation-based method was developed to probabilistically estimate the collision avoidance effect and injury mitigation effect of AEB and LDW assuming various near-miss situations leading to collisions. For the top 9 fatal traffic collision scenarios in Japan, the benefit of AEB and LDW in collision avoidance and injury mitigation was estimated quantitatively using this method.

REFERENCES

[1] Euro NCAP. Apr. 2021. "Euro NCAP AEB VRU Test Protocol v3.0.4." Internet: https://cdn.euroncap.com/media/62795/euro-ncap-aeb-vru-test-protocol-v304.pdf, Date Updated Nov. 2022

[2] Euro NCAP. July. 2019. "Euro NCAP LSS Test Protocol v3.0.2." Internet: https://cdn.euroncap.com/media/64973/euro-ncap-lss-test-protocol-v302.pdf. Date Updated Nov. 2022

[3] Euro NCAP. Apr. 2021. "Euro NCAP AEB Car-to-Car Test Protocol v3.0.3." Internet: https://cdn.euroncap.com/media/62794/euro-ncap-aeb-c2c-test-protocol-v303.pdf. Date Updated Nov. 2022

[4] Reßle, A., Lienkamp, M., & Fürst, F. 2011. "Method to Estimate the Field Effectiveness of an Automatic Braking System in Combination with an Adaptive Restraint System in Frontal Crashes." Proceedings of the 22nd ESV Conference

[5] Cabinet Office. Mar. 2018. "Research on analysis methods for estimating the effect of reducing traffic accident fatalities and injuries." Cross-ministerial Strategic Innovation Promotion Program

[6] Ministry of Economy, Trade and Industry. Mar. 2019. "Development and demonstration of simulation technology for estimating detailed effects of traffic accident reduction." Cross-ministerial Strategic Innovation Promotion Program

[7] Saito, Y., Inoue, H., & Raksincharoensak, P. 2018. "Safety Cushion: Potential Risk Estimation Based on Driving Context and Driving Behavior State (First Report)." Society of Automotive Engineers of Japan

[8] Yamamoto, A., Owaki, T., & Uesaka, K. 2011. "Analysis of differences in travel speed due to differences in bicycle riding space, etc." Japan Society of Civil Engineers

[9] Institute for Traffic Accident Research and Data Analysis. 2014. "Serious accidents involving four-wheeled vehicles traveling at low speeds when encountering two-wheeled vehicles." ITARDA INFORMATION No. 105

[10] Institute for Traffic Accident Research and Data Analysis. 2017. "Accidents between bicycles and four-wheeled vehicles." ITARDA INFORMATION No. 122

[11] Shikura, K. 2008. "Traffic Accident Case Study Analysis Study Group Analysis Study." Car Seminar, Vol.47, No. 11, 69-85

[12] Iwaki, R., Wakasugi, T., Teraoka, E. Y., Tanaka, S., & Uchida, N. 2013. "Analysis of driver response to road crossing pedestrian." Society of Automotive Engineers of Japan

[13] Iwaki, R., Wakasugi, T., Mochida, T., & Yoshida, S. 2013. "Modelling Lane Return Steering Behaviour When a Lane Departure Warning is Issued." Society of Automotive Engineers of Japan

[14] Yasuki, T., Kitagawa, Y., & Shigeta, K. 2009. "Development of next generation human body FE model capable of organ injury prediction." Proceedings of the 21st ESV Conference

[15] Euro NCAP. Oct. 2018. "Pedestrian Human Model Certification Version 1.1." Internet: https://cdn.euroncap.com/media/41783/tb-024-pedestrian-human-model-certification-v11.201811141155007002.pdf. Date Updated Nov. 2022

[16] Fischer, J. E., Bachmann, L. M., & Jaeschke, R. (2003). "A readers' guide to the interpretation of diagnostic test properties: clinical example of sepsis." Intensive Care Medicine.